

OPTIMAL AND ADAPTIVE ESTIMATION OF EXTREME VALUES IN THE PERMUTED MONOTONE MATRIX MODEL

Rong Ma¹, T. Tony Cai² and Hongzhe Li¹

Department of Biostatistics, Epidemiology and Informatics¹

Department of Statistics²

University of Pennsylvania

Philadelphia, PA 19104

Abstract

Motivated by applications in metagenomics, we consider the permuted monotone matrix model $Y = \Theta\Pi + Z$, where $Y \in \mathbb{R}^{n \times p}$ is observed, $\Theta \in \mathbb{R}^{n \times p}$ is an unknown signal matrix with monotone rows, $\Pi \in \mathbb{R}^{p \times p}$ is an unknown permutation matrix, and $Z \in \mathbb{R}^{n \times p}$ is the noise matrix. This paper studies the estimation of the extreme values associated to the signal matrix Θ , including its first and last columns, as well as their difference (the range vector). Treating these estimation problems as compound decision problems, minimax rate-optimal and adaptive estimators are constructed using spectral column sorting. Novel techniques that can be effective in estimating an arbitrary high-dimensional nonlinear operator are developed to establish minimax lower bounds, including generalized Le Cam's method and Fano's method. Numerical experiments using simulated and synthetic microbiome metagenomic data are presented, showing the superiority of the proposed methods over the alternatives. The methods are illustrated by comparing the growth rates of gut bacteria between inflammatory bowel disease patients and normal controls.

KEY WORDS: Compound decision problem; Extreme values; Minimax lower bounds; Monotone matrix; Permutation

1 Introduction

1.1 A permuted monotone matrix model in metagenomics studies

The statistical problem considered in this paper is motivated by the problem of estimating the bacterial growth dynamics using shotgun metagenomics data. Several methods have been developed to quantify the bacterial growth dynamics based on shotgun metagenomics data by extrapolating

particular patterns in the sequencing read coverages resulted from the bidirectional microbial DNA replications (Myhrvold et al., 2015; Abel et al., 2015; Korem et al., 2015; Brown et al., 2016). For bacterial species with known complete genome sequences, Korem et al. (2015) proposed to use the peak-to-trough ratio (PTR) of read coverages to quantify the bacterial growth rates after aligning the sequencing reads to the bacterial genomes. Besides quantifying the growth rates for the bacteria with complete genome sequences, it is also of great importance to estimate the growth rates of incomplete genome assemblies, where the coverages of contigs are observed in multiple samples. However, the order the contigs is only known up to an unknown permutation.

Gao and Li (2018) developed a computational algorithm (DEMIC) that accurately estimates the growth dynamics of a given assembled species by taking advantage of highly fragmented contigs assembled from multiple samples. DEMIC is based on the following permuted monotone matrix model:

$$Y = \Theta\Pi + Z \quad (1.1)$$

where the observed data $Y \in \mathbb{R}^{n \times p}$ is the matrix of the preprocessed contig coverage for a given bacterial species. Specifically, the entry Y_{ij} represents the log-transformed averaged read counts of the j -th contig of the bacterial species for the i -th sample after the preprocessing steps, including genome assemblies, GC adjustment of read counts and outlier filtering. The signal matrix $\Theta \in \mathbb{R}^{n \times p}$ represents the true log-transformed coverage matrix of n samples and p contigs, where each row is monotone due to the bi-directional replication of DNAs, $Z \in \mathbb{R}^{n \times p}$ is the noise matrix, and $\Pi \in \mathbb{R}^{p \times p}$ is a permutation matrix, corresponding to some permutation π from the symmetric group \mathcal{S}_p . Given the monotonicity constraint of the rows in Θ , the parameter space is defined as

$$\mathcal{D} = \left\{ \Theta = (\theta_{ij}) \in \mathbb{R}^{n \times p}, \pi \in \mathcal{S}_p : \begin{array}{l} \text{for each } 1 \leq i \leq n, \\ \text{either } \theta_{i,j} \leq \theta_{i,j+1} \text{ for all } j \\ \text{or } \theta_{i,j} \geq \theta_{i,j+1} \text{ for all } j \end{array} \right\}$$

where the rows of the matrix are required to be monotone.

As a result, under the permuted monotone matrix model, one can relate the two edge columns Θ_R and Θ_L to the log-transformed true peak and trough coverages over n samples and define their true log-PTRs as $\mathbf{R}(\Theta)$, where the two extreme columns Θ_R and Θ_L are the first and the last columns of Θ . The problem of estimating $\mathbf{R}(\Theta) = \Theta_R - \Theta_L$ (estimated log-PTRs, or ePTRs) from the Y was considered in Gao and Li (2018) and a computational algorithm was developed. The goal of this paper is to provide a rigorous statistical framework for optimal estimation of extreme values in the permuted monotone matrix model, including Θ_R and Θ_L and the range vector $\mathbf{R}(\Theta) = \Theta_R - \Theta_L$.

1.2 Related works

The permuted monotone matrix model (1.1) was previously studied in Ma et al. (2019a) where the focus is to optimally recover the underlying permutation π from Y . In particular, considering the loss function being either the 0-1 loss or the normalized Kendall's τ distance, a minimax optimal estimator is proposed and theoretically analyzed under various parameter spaces. In this paper, we investigate a related but different problem, of which the analysis requires novel insights of the model.

Model (1.1) is related to the shape constrained matrix denoising model studied in the isotonic regression literature. Specifically, risk bounds and a rate-optimal estimator for Θ under Frobenius norm with known $\Pi = \mathbf{I}_p$ were obtained in Chatterjee et al. (2015) for $n = 1$ and later in Chatterjee et al. (2018) for general $n > 1$. For the cases with unknown permutation Π , the minimax rate for estimating Θ and $\Theta\Pi$ under the Frobenius norm was studied in a recent paper of Flammarion et al. (2019), under the name of statistical seriation, a model that has a similarity to our model (1.1).

Model (1.1) also has connections to the uncoupled isotonic regression, where in addition to the monotonicity constraint of the regression function, the sample labels of the covariates and the outcome are unknown. In fact, model (1.1) can be treated as a multivariate extension of the uncoupled isotonic regression with fixed designs. For the univariate cases, Carpentier and Schlueter (2016) studied nonparametric estimation of smooth regression functions using a deconvolution approach. More recently, using the idea of optimal transport, a minimax optimal estimator of the underlying signals under the Wasserstein distance was obtained in Rigollet and Weed (2018) (see also Mao et al. (2018) and references therein). However, these studies focus on the estimation of the underlying signal matrix Θ or $\Theta\Pi$, whereas the quantities of interest in the current study are the extreme columns. As will be seen later, these two problems are fundamentally different.

1.3 Main contributions

The main contributions of the paper can be summarized as follows.

- *Minimax optimal and adaptive estimation.* Based on the idea of spectral column sorting and the theory of low-rank matrix estimation, we develop rate-optimal adaptive estimators for the extreme columns and the range vector. In particular, the minimax optimality of the proposed methods are theoretically established and empirically illustrated with numerical experiments, which also justify its applicability in analyzing real datasets such as the microbiome metagenomics data.
- *Novel minimax lower bound techniques.* In order to obtain asymptotically sharp minimax lower bounds associated with the estimation problems, we develop novel technical tools that generalize Le Cam's method and Fano's method (Yu, 1997), respectively, by considering

testing two or multiple composite/fuzzy hypotheses posed on the parameter spaces. These general lower bounds (Lemmas 2.1 and 2.2) can be of independent interest by providing an effective estimation of an arbitrary high-dimensional (nonlinear) operator.

- *Insights on the compound decision problems.* As estimating an extreme column consists of simultaneous consideration of n estimation problems having identical formal structure across the n coordinates, the problem is essentially a compound statistical decision problem (Robbins, 1951, 1964). Comparing our proposed estimators with some alternatives, we provide strong theoretical and empirical evidences that, in general, for a compound decision problem, an optimal rule should also be “compound” rather than “simple” (see Section 2.2 for their explicit definitions).

1.4 Organization and notation

The rest of the paper is organized as follows. In Section 2, we propose a spectral estimator, provide its risk upper bounds, and establish the minimax rates of convergence in certain parameter spaces. Optimal adaptive estimation of the range vector is considered in Section 3. In Section 4, alternative estimators are discussed and evaluated theoretically. Numerical studies are presented in Section 5, where we consider simulations based on both the model-generated data and a synthetic microbiome metagenomic dataset, demonstrating the empirical superiority of our proposed methods over the alternative/existing methods. We also analyze a real metagenomic dataset to illustrate our method. Section 6 discusses our theoretical conditions and possible extensions. For reasons of space, we prove Theorems 2.3 and 4.1 in Section 7 and defer the proofs of other theorems and technical lemmas to the Supplementary Material (Ma et al., 2019b).

Throughout our paper, we define the permutation π as a bijection from the set $\{1, 2, \dots, p\}$ onto itself. For simplicity, we denote $\pi = (\pi(1), \pi(2), \dots, \pi(p))$. All permutations of the set $\{1, 2, \dots, p\}$ form a symmetric group, equipped with the function composition operation \circ , denoted as \mathcal{S}_p . For any $\pi \in \mathcal{S}_p$, we denote $\pi^{-1} \in \mathcal{S}_p$ as its group inverse, so that $\pi \circ \pi^{-1} = \pi^{-1} \circ \pi = id$. In particular, we may use π and its corresponding permutation matrix $\Pi \in \mathbb{R}^{p \times p}$ interchangeably, depending on the context. For a vector $\mathbf{a} = (a_1, \dots, a_n)^\top \in \mathbb{R}^n$, we define the ℓ_p norm $\|\mathbf{a}\|_p = (\sum_{i=1}^n |a_i|^p)^{1/p}$, and the ℓ_∞ norm $\|\mathbf{a}\|_\infty = \max_{1 \leq j \leq n} |a_j|$. For a matrix $\Theta \in \mathbb{R}^{p_1 \times p_2}$, we denote $\Theta_{\cdot i} \in \mathbb{R}^{p_1}$ as its i -th column and denote $\Theta_{i \cdot} \in \mathbb{R}^{p_2}$ as its i -th row. We write $a \wedge b = \min\{a, b\}$ and $a \vee b = \max\{a, b\}$. Furthermore, for sequences $\{a_n\}$ and $\{b_n\}$, we write $a_n = o(b_n)$ if $\lim_n a_n/b_n = 0$, and write $a_n = O(b_n)$, $a_n \lesssim b_n$ or $b_n \gtrsim a_n$ if there exists a constant C such that $a_n \leq Cb_n$ for all n . We write $a_n \asymp b_n$ if $a_n \lesssim b_n$ and $a_n \gtrsim b_n$. Lastly, C, C_0, C_1, \dots are constants that may vary from place to place.

2 Minimax Optimal Extreme Column Estimation

2.1 Extreme column localization via spectral sorting

We begin studying minimax optimal extreme column estimation by constructing a spectral estimator. A crucial step for estimating the extreme columns is to sort the permuted columns in order to identify the extreme ones. Toward this end, for any $\Theta \in \mathcal{D}$, we consider the row-centered matrix

$$\Theta' = \Theta \left(\mathbf{I}_p - \frac{1}{p} \mathbf{e} \mathbf{e}^\top \right) \in \mathbb{R}^{n \times p}, \quad (2.1)$$

where $\mathbf{e} = (1, \dots, 1)^\top \in \mathbb{R}^p$. Intuitively, Θ' is invariant to the row averages of Θ and preserves the row-monotonicity structure as well as the distances between the columns of Θ . The singular value decomposition (SVD) of Θ' can be written as

$$\Theta' = \sum_{i=1}^r \lambda_i \mathbf{u}_i \mathbf{v}_i^\top, \quad \text{for some } r \leq \min\{n, p\}, \quad (2.2)$$

where $\lambda_1 \geq \lambda_2 \geq \dots \geq \lambda_r$ are the ordered singular values of Θ' and \mathbf{u}_i and \mathbf{v}_i are the right and left singular vectors corresponding to λ_i , respectively. To overcome the identifiability issue, we assume

(A) λ_1 has multiplicity one and the first nonzero component of \mathbf{v}_1 is negative.

The following proposition, whose original version was obtained by Ma et al. (2019a) for the purpose of recovering the underlying permutation π , provides an important insight that the row-monotonicity of a matrix actually implies the monotonicity of the components of its leading right singular vector \mathbf{v}_1 . This property plays a fundamental role in analyzing the permuted monotone matrix model.

Proposition 2.1. *Under assumption (A), let Θ' be defined as above (2.1), then its first right singular vector $\mathbf{v}_1 = (v_{11}, \dots, v_{1p})^\top$ is a centered monotone vector, i.e., $\sum_{i=1}^p v_{1i} = 0$ and $v_{11} \leq v_{12} \leq \dots \leq v_{1p}$. In addition, the sign vector $\text{sgn}(\mathbf{u}_1)$ indicates the direction of monotonicity of the rows of Θ' (or Θ).*

From the above proposition, the relative orders of the columns of Θ' (and Θ) are qualitatively preserved by the leading right singular vector \mathbf{v}_1 , whereas the directions of monotonicity for different rows are coded by the leading left singular vector \mathbf{u}_1 . As a result, given a column-permuted and noisy matrix Y in (1.1), one could localize the extreme columns Θ_R and Θ_L in $\Theta\Pi$ by considering the row-normalized observation matrix $X = Y(\mathbf{I}_p - \frac{1}{p} \mathbf{e} \mathbf{e}^\top)$ and its first left singular vector, i.e.,

$$\hat{\mathbf{v}} = (\hat{v}_1, \dots, \hat{v}_p)^\top = \arg \max_{\mathbf{v} \in \mathbb{R}^p: \|\mathbf{v}\|_2=1} \mathbf{v}^\top X^\top X \mathbf{v}. \quad (2.3)$$

In light of Proposition 2.1, Ma et al. (2019a) showed that the order statistics $\{\hat{v}_{(1)}, \dots, \hat{v}_{(p)}\}$ can

be used to optimally recover the permutation π , or the original column orders, by tracing back the permutation map between the elements of $\hat{\mathbf{v}}$ and their order statistics. Clearly, for extreme column localization, the two extreme values $\hat{v}_{(1)}$ and $\hat{v}_{(p)}$ are more relevant. In fact, it is shown in the subsequent section and Section 4.1 that, a minimax optimal and adaptive procedure can be constructed using such spectral quantities.

2.2 Compound decision problem and the minimax optimal estimators

To study the problem of optimal estimation of the extreme columns Θ_L and Θ_R , for any estimator $\hat{\Theta}_\ell \in \mathbb{R}^n$ with $\ell \in \{R, L\}$, we consider the normalized ℓ_2 distances $\frac{1}{\sqrt{n}}\|\hat{\Theta}_\ell - \Theta_\ell\|_2$ and denote the corresponding estimation risk as

$$\mathcal{R}_\ell(\hat{\Theta}_\ell) = \frac{1}{\sqrt{n}}\mathbb{E}\|\hat{\Theta}_\ell - \Theta_\ell\|_2. \quad (2.4)$$

For some parameter space \mathcal{F} , we define the minimax risks as

$$\inf_{\hat{\Theta}_\ell} \sup_{\mathcal{F}} \mathcal{R}_\ell(\hat{\Theta}_\ell),$$

and define the minimax optimal estimator as $\hat{\Theta}_\ell^*$ in the sense that

$$\sup_{\mathcal{F}} \mathcal{R}_\ell(\hat{\Theta}_\ell^*) \asymp \inf_{\hat{\Theta}_\ell} \sup_{\mathcal{F}} \mathcal{R}_\ell(\hat{\Theta}_\ell).$$

In general, the problem of estimating Θ_ℓ consists of n individual sub-problems, namely, estimating each of its n coordinates. Following the concept proposed by Robbins (1951, 1964) and further elaborated in Samuel (1967); Copas (1969); Zhang (2003) and Brown and Greenshtein (2009), among many others, we observe that the problem of finding a minimax optimal estimator $\hat{\Theta}_\ell^*$ is a compound statistical decision problem, as the n individual sub-problems are amalgamated into one larger problem through the combined risk (2.4). However, although the observations over n samples are independent, it has been argued that, in general, for a compound decision problem, usually the *simple rules/estimators*, where only the i -th sample is used to estimate the i -th coordinate, are suboptimal, whereas a minimax optimal estimator should be *compound* in the sense that multiple samples are used for the estimation of each coordinate.

In light of our discussion in Section 2.1 as to the fundamental role of $(\lambda_1, \mathbf{u}_1, \mathbf{v}_1)$, throughout we will consider the cases where Θ' is *approximately rank-one* in the sense that $\Theta' \approx \lambda_1 \mathbf{u}_1 \mathbf{v}_1^\top$ (see Section 2.3 for the precise characterization). Although we restrict our attention the approximate rank-one cases for simplicity, we emphasize that (i) strong technicality and rich mathematical structures already exist in such cases, and (ii) the class of approximately rank-one matrices is usually flexible enough in modeling the real-world data such as our motivating example from the

microbiome metagenomics.

Now we introduce our proposed minimax optimal and adaptive estimators for the extreme columns as

$$\hat{\Theta}_R^* = \hat{v}_{(p)} X \hat{\mathbf{v}} + \frac{1}{p} Y \mathbf{e} \in \mathbb{R}^n, \quad \hat{\Theta}_L^* = \hat{v}_{(1)} X \hat{\mathbf{v}} + \frac{1}{p} Y \mathbf{e} \in \mathbb{R}^n, \quad (2.5)$$

where we recall that $\hat{\mathbf{v}}$ is defined in (2.3) and $\hat{v}_{(i)}$ is the i -th smallest order statistic among $\{\hat{v}_1, \dots, \hat{v}_p\}$. By construction, the proposed estimators (2.5) are compound estimators, and each of them consists of two parts: the first part estimates the extreme columns of the row-centered matrix Θ' whereas the second part compensates the row-specific mean effects. In particular, to construct the first parts of $\hat{\Theta}_R^*$ and $\hat{\Theta}_L^*$, the first-order approximation $\Theta'_{\ell} \approx \lambda_1 v_{1\ell} \mathbf{u}$ for $\ell = 1$ and p is incorporated with $v_{1\ell}$ being estimated by $\hat{v}_{(\ell)}$ and $\lambda_1 \mathbf{u}_1$ being estimated by $X \hat{\mathbf{v}}$.

2.3 Risk upper bounds

In this section, we study the theoretical properties of our proposed estimator $\hat{\Theta}_R^*$ by considering its pointwise risks $\mathcal{R}_R(\hat{\Theta}_R^*)$ for some fixed $\Theta \in \mathcal{D}$, and the uniform risk $\sup_{\mathcal{F}} \mathcal{R}_R(\hat{\Theta}_R^*)$ over some parameter space \mathcal{F} to be specified later. Similar results for estimating Θ_L hold by symmetry. To simplify notations, we define the rate function

$$\psi = \psi(n, p) = \sqrt{\frac{\log p}{n}} + \frac{1}{\sqrt{p}}. \quad (2.6)$$

The following theorem concerns the pointwise risk upper bound of our proposed estimator $\hat{\Theta}_R^*$ over \mathcal{D} .

Theorem 2.1 (Pointwise Upper Bounds). *For any $\Theta \in \mathbb{R}^{n \times p}$ satisfying (A), recall that the SVD of its row-centered matrix Θ' is given by (2.2). Assume that $(\Theta, \pi) \in \mathcal{D}$, the noise matrix Z has i.i.d. entries $Z_{ij} \sim N(0, \sigma^2)$ and $\sum_{i=2}^r \lambda_i \leq \sigma \sqrt{\log p}$. Then*

$$\mathcal{R}_R(\hat{\Theta}_R^*) \lesssim \left(\frac{\lambda_1 v_{1p}}{\sqrt{n}} + \sigma \sqrt{\log(pn)} \right) \left(\frac{\sigma \sqrt{(\lambda_1^2 + \sigma^2 p)n}}{\lambda_1^2 - \lambda_2^2} \wedge 1 \right) + \sigma \psi. \quad (2.7)$$

In addition, if $\lambda_1^2 \gtrsim \sigma^2 n \log(np) \left(\frac{1}{v_{1p}^2} \wedge \frac{1}{\psi^2} + \frac{1}{\psi} \sqrt{\frac{p}{n \log(pn)}} \right)$, we have

$$\mathcal{R}_R(\hat{\Theta}_R^*) \lesssim \frac{v_{1p} \lambda_1}{\sqrt{n}} \left(\frac{\sigma \sqrt{(\lambda_1^2 + \sigma^2 p)n}}{\lambda_1^2} \wedge 1 \right) + \sigma \psi. \quad (2.8)$$

Remark 2.1. From the above theorem, the conditions $\sum_{i=2}^r \lambda_i \leq \sigma \sqrt{\log p}$ and $\lambda_1^2 \gtrsim \sigma^2 n \log(np) (v_{1p}^{-2} \wedge \psi^{-2} + \psi^{-1} \sqrt{\frac{p}{n \log(pn)}})$ essentially imply the first-order approximation $\Theta' \approx \lambda_1 \mathbf{u}_1 \mathbf{v}_1^\top$. Consequently, these conditions amount to removing the factor $\sigma \sqrt{\log(pn)}$ and rounding the spectral gap $\lambda_1^2 - \lambda_2^2 \approx$

λ_1^2 in the first component of the upper bound (2.7). The simplified upper bound (2.8) is more interesting in the sense that it will lead to asymptotically sharp minimax rate of convergence over certain parameter spaces to be specified later.

Remark 2.2. The risk upper bound (2.8) consists of two components. In light of our theoretical analysis, in the first component, the factor $(\sigma\sqrt{(\lambda_1^2 + \sigma^2 p)n}/\lambda_1^2 \wedge 1)$ is the error due to estimating the leading right singular vector \mathbf{u}_1 by its sample counterpart, whereas the factor $v_{1p}\lambda_1/\sqrt{n}$ reflects the overall magnitude of the extreme column Θ_R . Within the second component $\sigma\psi(n, p)$, the term $\sigma\sqrt{\log p/n}$ comes from using the order statistic $\hat{v}_{(p)}$ to estimate the largest component of \mathbf{v}_1 , whereas the term σ/\sqrt{p} is the error due to estimating the row specific averaged signals by $\frac{1}{p}Y\mathbf{e}$.

Remark 2.3. The factor $(\sigma\sqrt{(\lambda_1^2 + \sigma^2 p)n}/\lambda_1^2 \wedge 1)$ in the risk upper bound (2.8) suggests a phase transition around $\lambda_1^2 = \sigma^2(n + \sqrt{np})$. From the theory of low-rank matrix estimation (Cai and Zhang, 2018), the quantity $\sigma^2(n + \sqrt{np})$ is the critical point for λ_1^2 , below which it is impossible to estimate the singular vector \mathbf{u}_1 . Such a critical point plays an important role in our subsequent analysis.

Based on the pointwise risk upper bound in Theorem 2.1, we can further derive the uniform risk upper bounds for our proposed estimators over a sequence of indexed parameter spaces. Specifically, with respect to the SVD given by (2.2) and the conditions of Theorem 2.1, we define the following indexed parameter space

$$\mathcal{D}_R(t, \beta) = \left\{ (\Theta, \pi) \in \mathcal{D} : \begin{array}{l} \text{(A) holds, } 0 \leq v_{1p} \leq \beta, \\ \lambda \in [t/8, 8t], \sum_{i=2}^r \lambda_i \leq \sigma\sqrt{\log p} \end{array} \right\}, \quad (2.9)$$

with $t \geq 0$ and $p^{-1/2} \leq \beta \leq 1$. Here the constraint on β is natural since \mathbf{v}_1 is a unit vector and β is no less than the order of its largest component. Intuitively, the hyper-parameters (t, β) characterize the global signal strength as well as the relative position of the extreme column Θ_R shared by the signal matrices in $\mathcal{D}_R(t, \beta)$.

Theorem 2.2 (Uniform Upper Bound). *Suppose the pair (t, β_R) satisfies $p^{-1/2} \leq \beta_R \leq 1$, $t^2 \gtrsim \sigma^2 n \log(np) \left(\frac{1}{\beta_R^2} \wedge \frac{1}{\psi^2} + \frac{1}{\psi} \sqrt{\frac{p}{n \log(pn)}} \right)$ and the noise matrix Z has i.i.d. entries $Z_{ij} \sim N(0, \sigma^2)$. Then we have*

$$\sup_{\mathcal{D}_R(t, \beta_R)} \mathcal{R}_R(\hat{\Theta}_R^*) \lesssim \frac{\beta_R t}{\sqrt{n}} \left(\frac{\sigma\sqrt{(t^2 + \sigma^2 p)n}}{t^2} \wedge 1 \right) + \sigma\psi. \quad (2.10)$$

Remark 2.4. In the above theorem, again there is a phase transition for the first component of

the risk upper bound when t^2 passes $\sigma^2(n + \sqrt{np})$. Specifically, in (2.10)

$$\frac{\beta_R t}{\sqrt{n}} \left(\frac{\sigma \sqrt{(t^2 + \sigma^2 p)n}}{t^2} \wedge 1 \right) \asymp \begin{cases} \frac{\beta_R t}{\sqrt{n}} & \text{if } t^2 \lesssim \sigma^2(n + \sqrt{np}), \\ \frac{\beta_R \sigma \sqrt{t^2 + \sigma^2 p}}{t} & \text{if } t^2 \gtrsim \sigma^2(n + \sqrt{np}). \end{cases}$$

The dichotomy around $\sigma^2(n + \sqrt{np})$ is originated from the factor $(1 \wedge \sigma \sqrt{(\lambda_1^2 + \sigma^2 p)n}/\lambda_1^2)$ in the pointwise risk bound (2.8).

The difference in the performance of $\hat{\Theta}_R^*$ over the regions $t^2 \gtrsim \sigma^2(n + \sqrt{np})$ and $t^2 \lesssim \sigma^2(n + \sqrt{np})$ is distinguished by the first component of the risk upper bound. Intuitively, from Remark 2.4, the collection of parameter spaces $\{\mathcal{D}_R(t, \beta_R) : t^2 \leq \sigma^2(n + \sqrt{np})\}$ depicts the theoretical performance of $\hat{\Theta}_R^*$ over the “weak signal-to-noise ratio” regime, while the collection $\{\mathcal{D}_R(t, \beta_R) : t^2 \geq \sigma^2(n + \sqrt{np})\}$ describes the performance of $\hat{\Theta}_R^*$ over the “strong signal-to-noise ratio” regime.

2.4 Minimax lower bound, optimality and adaptivity

In this section, we establish the minimax rate of convergence and the optimality of our proposed estimators over the parameter space $\mathcal{D}_R(t, \beta_R)$. The following theorem concerns the minimax lower bound of the risk.

Theorem 2.3 (Minimax Lower Bound). *Suppose Z in model (1.1) has i.i.d. entries $Z_{ij} \sim N(0, \sigma^2)$. Then, for sufficiently large (n, p) and any $\mathcal{D}_R(t, \beta)$ such that $t^2 \geq c_0 \left(\frac{1 - \beta_R^2}{\beta_R^2} \sigma^2 n \psi^2 \vee \frac{\beta_R^2}{1 - \beta_R^2} \sigma^2 p \right)$ and $c_1 p^{-1/2} \sqrt{\log p} \leq \beta_R \leq c_2$ for some constants $c_0, c_1 > 0$ and $0 < c_2 < 1$,*

$$\inf_{\hat{\Theta}_R} \sup_{\mathcal{D}_R(t, \beta_R)} \mathcal{R}_R(\hat{\Theta}_R) \gtrsim \frac{\beta_R t}{\sqrt{n}} \left(\frac{\sigma \sqrt{(t^2 + \sigma^2 p)n}}{t^2} \wedge 1 \right) + \sigma \psi. \quad (2.11)$$

Remark 2.5. In the above theorem, some additional conditions are posed in order to obtain the minimax lower bound. Specifically, the matching lower bound (2.11) over $\mathcal{D}_R(t, \beta_R)$ is obtained under the constraint $t^2 \geq c_0 \left(\frac{1 - \beta_R^2}{\beta_R^2} \sigma^2 n \psi^2 \vee \frac{\beta_R^2}{1 - \beta_R^2} \sigma^2 p \right)$, which is effective only when $t^2 = o(\sigma^2 p)$. In addition, for the minimax lower bound, there is an extra factor $\sqrt{\log p}$ required for the lower bound condition of β_R , which is due to our specific analytical constructions in our proofs. Here we do not aim to optimize these technical conditions, but we argue that these conditions are reasonably weak and certain relaxation might be possible yet technically challenging.

In general, the proof of Theorem 2.3 is involved. The main difficulty lies on the non-linearity and multi-dimensionality of the maps from the original parameter Θ to its extreme columns of interest. As the lower bound contains many components, we essentially derived four minimax lower bounds corresponding to different worst-case scenarios with their respective emphases (see Section 7 for more details). In addition to the existing techniques for proving minimax lower bounds

such as the Varshamov-Gilbert bound (Lemma 7.3) and the sphere packing of the Grassmannian manifolds (Lemma 7.4), the following two novel lower bound techniques were developed to facilitate the proofs.

Lemma 2.1 (Generalized Le Cam's Method). *Let μ_0 and μ_1 be two priors on the parameter space Θ of the family $\{P_\theta\}$, and let P_j be the posterior probability measures on $(\mathcal{X}, \mathcal{A})$ such that*

$$P_j(S) = \int P_\theta(S) \mu_j(d\theta), \quad \forall S \in \mathcal{A}, \quad j = 0, 1.$$

Let $F : \Theta \rightarrow (\mathbb{R}^d, d)$. If (i) there exist $F_0 \in \mathbb{R}^d$ and a $2s$ -ball $\mathbb{B}_d(F_0, 2s)$ centered at F_0 such that $\mu_0(\theta \in \Theta : F(\theta) = F_0) = 1$, $\mu_1(\theta \in \Theta : F(\theta) \notin \mathbb{B}_d(F_0, 2s)) = 1$, and (ii) $\chi^2(P_1, P_0) \leq \alpha < \infty$, then

$$\inf_{\hat{F}} \sup_{\theta \in \Theta} P_\theta(d(\hat{F}, F(\theta)) \geq s) \geq \max \left\{ \frac{e^{-\alpha}}{4}, \frac{1 - \sqrt{\alpha/2}}{2} \right\}.$$

Lemma 2.2 (Generalized Fano's Method). *Let $\mu_0, \mu_1, \dots, \mu_M$ be $M + 1$ priors on the parameter space Θ of the family $\{P_\theta\}$, and let P_j be the posterior probability measures on $(\mathcal{X}, \mathcal{A})$ such that*

$$P_j(S) = \int P_\theta(S) \mu_j(d\theta), \quad \forall S \in \mathcal{A}, \quad j = 0, 1, \dots, M.$$

Let $F : \Theta \rightarrow (\mathbb{R}^d, d)$. If (i) there exist some sets $B_0, B_1, \dots, B_M \subset \mathbb{R}^d$ such that $d(B_i, B_j) \geq 2s$ for some $s > 0$ for all $0 \leq i, j \leq M$ and $\mu_j(\theta \in \Theta : F(\theta) \in B_j) = 1$, and (ii) $\frac{1}{M} \sum_{j=1}^M D(P_j, P_0) \leq \alpha \log M$ with $0 < \alpha < 1/8$, then

$$\inf_{\hat{F}} \sup_{\theta \in \Theta} P_\theta(d(\hat{F}, F(\theta)) \geq s) \geq \frac{\sqrt{M}}{1 + \sqrt{M}} \left(1 - 2\alpha - \sqrt{\frac{2\alpha}{\log M}} \right).$$

Remark 2.6. The above lemmas concern testing two and multiple composite hypotheses about an arbitrary operator $F : \Theta \rightarrow (\mathbb{R}^d, d)$ defined on some parameter space Θ , which generalize the classical Le Cam's method and the Fano's method (Yu, 1997; Tsybakov, 2009), as well as the ideas of Cai and Low (2011). The proofs of these lemmas can be found in the Supplementary Material (Ma et al., 2019b).

Combining the upper and the lower bound results, we obtain the exact minimax rate of convergence for estimating Θ_R . Specifically, under the conditions of Theorem 2.2 and Theorem (2.3), we have

$$\inf_{\hat{\Theta}_R} \sup_{\mathcal{D}_R(t, \beta_R)} \mathcal{R}_R(\hat{\Theta}_R) \asymp \frac{\beta_R t}{\sqrt{n}} \left(\frac{\sigma \sqrt{(t^2 + \sigma^2 p)n}}{t^2} \wedge 1 \right) + \sigma \psi. \quad (2.12)$$

As a consequence of the phase transition phenomena pointed out in Remark 2.3 and 2.4, some interesting insights about the interplay between the global signal strength t^2 , the dimensionality

of the problem as reflected by the ratio p/n , the hardness of estimating Θ_R and that of estimating the leading left singular vector \mathbf{u}_1 , can be obtained from (2.12). Specifically, under the high-dimensional setting where $p/n > 1$, (i) within the weak signal-to-noise ratio regime ($t^2 \lesssim \sigma^2 \sqrt{np}$), since estimating \mathbf{u}_1 is impossible, the best estimator of Θ_R can only benefit from reducing the overall signal strength t^2 ; (ii) within the intermediate signal-to-noise ratio regime ($\sigma^2 \sqrt{np} \lesssim t^2 \lesssim \sigma^2 p$), as now it is possible to estimate \mathbf{u}_1 , increasing the signal strength t^2 will reduce the difficulty of estimating \mathbf{u}_1 and therefore the rate of estimating Θ_R ; (iii) within the strong signal-to-noise ratio regime ($t^2 \gtrsim \sigma^2 p$), while \mathbf{u}_1 can be even better estimated, the difficulty of estimating Θ_R will no longer be reduced as the benefit is neutralized by the increased signal strength t^2 . In contrast, under the low- to moderate-dimensional setting where $p/n < 1$, (i) when $t^2 \lesssim \sigma^2 n$, similar phenomena can be observed as under the high-dimensional setting where $t^2 \lesssim \sigma^2 \sqrt{np}$; (ii) once the signal strength t^2 passes the threshold $\sigma^2 n$, neither t^2 nor the hardness of estimating \mathbf{u}_1 will effect the estimation of Θ_R , as the optimal rate in this case is of order $\sigma \beta_R$. Especially, all the above rate analysis is subjected to a possible lower bound of $\psi(n, p)$. See Figure 1 for an illustration.

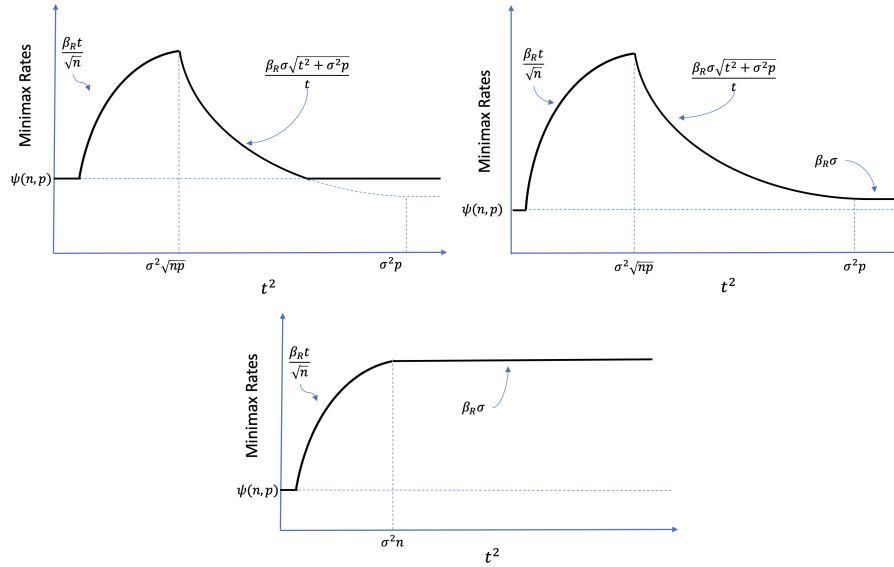


Figure 1: A graphical illustration of the minimax risks over $\mathcal{D}_R(t, \beta_R)$ as a function of t^2 when $p > n$ (top) and $p < n$ (bottom). The upper left and right plots correspond to $\beta_R \lesssim \psi(n, p)$ and $\beta_R \gtrsim \psi(n, p)$, respectively.

Moreover, as the above minimax optimal rates are simultaneously attained by our proposed estimator $\hat{\Theta}_R^*$, regardless of the specific underlying indices (t, β_R) , we conclude that $\hat{\Theta}_R^*$ is minimax rate-adaptive over the collection of parameter spaces

$$\{\mathcal{D}_R(t, \beta_R) : t^2 \geq c_0 q(\beta_R, n, p), p^{-1/2} c_1 \sqrt{\log p} \leq \beta_R \leq c_2 < 1\},$$

where $q(\beta_R, n, p) = \sigma^2 n \log(np) \left(\frac{1}{\beta_R^2} \wedge \frac{1}{\psi^2} + \frac{1}{\psi} \sqrt{\frac{p}{n \log(pn)}} \right) + \left(\frac{1 - \beta_R^2}{\beta_R^2} \sigma^2 n \psi^2 + \frac{\beta_R^2 \sigma^2 p}{1 - \beta_R^2} \right)$.

2.5 Special case: the permuted linear growth model

In the previous section, theoretical results have been obtained for the general approximately rank-one cases characterized by (2.9) as well as the conditions of Theorem 2.1 and 2.2. One advantage is the rich row-monotonicity structures contained in such parameter spaces, which adapts well to real applications such as our motivating example in microbiome studies where the noisy datasets are generated from the shotgun metagenomic sequencing (Boulund et al., 2018; Gao and Li, 2018). However, in many cases (such as classical theories of the bacterial growth dynamics), an important subclass of the general permuted monotone matrix model has usually been considered for its heuristic simplicity and explanatory power. Following Ma et al. (2019a), we refer this sub-model as the *permuted linear growth model*, where (1.1) holds over the restricted set

$$\mathcal{D}_0 = \left\{ (\Theta, \pi) \in \mathcal{D} : \begin{array}{l} \theta_{ij} = a_i \eta_j + b_i, \text{ where } a_i, b_i \in \mathbb{R} \text{ for } 1 \leq i \leq n, \\ \eta_j \leq \eta_{j+1} \text{ for } 1 \leq j \leq p-1 \text{ and } \sum_{j=1}^p \eta_j = 0. \end{array} \right\}.$$

In other words, each row of Θ has a linear growth pattern with possibly different intercepts and slopes. In contrast to the “linear growth model” considered in Ma et al. (2019a), for each row of Θ , we allow it to be either monotonic increasing or decreasing, depending on the sign of a_i . Denote $\mathbf{a} = (a_i)_{1 \leq i \leq n}$, $\boldsymbol{\eta} = (\eta_j)_{1 \leq j \leq p}$ and $\mathbf{b} = (b_i)_{1 \leq i \leq n}$. In this case, the extreme columns of interest have the forms of $\Theta_R = \mathbf{a}\eta_p$ and $\Theta_L = \mathbf{a}\eta_1$.

Remark 2.7. In relation to our motivating examples, in the context of bacterial growth dynamics, the above model is sometimes referred as the Cooper-Helmstetter model (Cooper and Helmstetter, 1968; Bremer and Churchward, 1977) that associates the copy number of genes with their relative distances to the replication origin. Specifically, a_i is the ratio of genome replication time and doubling time for the i th sample, η_j is the distance from the replication origin for the j th contig, and b_i is related to the read counts at the replication origin and the sequencing depth. Consequently, the extreme columns $\mathbf{a}\eta_p$ and $\mathbf{a}\eta_1$ correspond to the true log-transformed peak and trough coverages that are used to quantify the bacterial growth dynamics across the samples (see also Section 5.2 and 5.3 for more details).

The SVD (2.2) for $\Theta \in \mathcal{D}_0$ has a reduced form. Specifically, the row-centered matrix Θ' is exactly rank-one, where the leading right singular vector \mathbf{v}_1 has components

$$v_{1j} = \frac{\eta_j}{\|\boldsymbol{\eta}\|_2}, \quad \text{for } j = 1, \dots, p, \quad (2.13)$$

and the largest singular value admits the expression

$$\lambda_1 = \|\mathbf{a}\|_2 \|\boldsymbol{\eta}\|_2. \quad (2.14)$$

Intuitively, the set $\{v_{1j}\}_{1 \leq j \leq p}$ characterize the exact normalized column positions of Θ' (and Θ),

while λ_1 summarizes the slope magnitude of the rows and the overall separateness of the columns.

Consequently, the risk upper bounds of Theorem 2.1 has a reduced form with some simpler and more intuitive statistical interpretations. Specifically, consider the pointwise risk upper bound (2.8). On the one hand, when λ_1 is large in the sense that $\lambda_1^2 \gtrsim \sigma^2(n + \sqrt{np})$, we have

$$\mathcal{R}_R(\hat{\Theta}_R^*) \lesssim \frac{\sigma\eta_p}{\|\boldsymbol{\eta}\|_2} \sqrt{1 + \frac{\sigma^2 p}{\|\mathbf{a}\|_2^2 \|\boldsymbol{\eta}\|_2^2}} + \sigma\psi. \quad (2.15)$$

In this case, as the signal differences between every consecutive columns are steep enough so that the slopes \mathbf{a} can be well estimated, increasing $\|\boldsymbol{\eta}\|_2$ or $\|\mathbf{a}\|_2$ would expand the advantage and therefore leads to a better estimate. However, when $\lambda_1^2 \lesssim \sigma^2(n + p)$, the upper bound becomes

$$\mathcal{R}_R(\hat{\Theta}_R^*) \lesssim \frac{\sigma\eta_p}{\|\boldsymbol{\eta}\|_2} + \sigma\psi. \quad (2.16)$$

In the case, the advantage of large $\|\mathbf{a}\|_2$ has been exploited to its extreme so that increasing $\|\mathbf{a}\|_2$ will no longer improve the performance of $\hat{\Theta}_R^*$.

On the other hand, if $\lambda_1^2 \lesssim \sigma^2(n + \sqrt{np})$, we have

$$\mathcal{R}_R(\hat{\Theta}_R^*) \lesssim \frac{\|\mathbf{a}\|_2 \eta_p}{\sqrt{n}} + \sigma\psi, \quad (2.17)$$

where the first term is proportional to the overall slope magnitude $\|\mathbf{a}\|_2$, but does not rely on the locations of the other columns, i.e., η_j for $1 \leq j \leq p-1$. In this case, since the signal changes across different columns are so vague, $\hat{\Theta}_R^*$ fails to implement a good estimate for the slopes \mathbf{a} and the estimation error can only decrease when the extreme column $\Theta_R = \mathbf{a}\eta_p$ itself (and its norm $\|\mathbf{a}\|_2 \eta_p$) is close to zero. Comparing the rates from (2.15) to (2.17), we can see an interesting phenomena as to the discrepant role played by the overall slope measure $\|\mathbf{a}\|_2$. In general, the theoretical performance of $\hat{\Theta}_R^*$ is clearly driven by the global signal-to-ratio $\lambda_1^2/\sigma^2 = \|\mathbf{a}\|_2^2 \|\boldsymbol{\eta}\|_2^2/\sigma^2$, which directly measures the magnitude of the signal changes or the degree of monotonicity relative to the noise level.

Following the same argument as the proof of Theorem 2.3, it can be shown that the same minimax lower bounds hold over some indexed parameter spaces in \mathcal{D}_0 , which along with Theorem 2.2 implies the same minimax rates. Specifically, if we define the indexed parameter space $\mathcal{D}_{0,R}(t, \beta) = \{(\Theta, \pi) \in \mathcal{D}_0 : 0 \leq \eta_p/\|\boldsymbol{\eta}\|_2 \leq \beta, \|\mathbf{a}\|_2 \|\boldsymbol{\eta}\|_2 \in [t/8, 8t]\}$, then one can similarly show that for any pair (t, β_R) such that $t^2 \gtrsim q(\beta_R, n, p)$ and $p^{-1/2} \sqrt{\log p} \lesssim \beta_R \leq c < 1$, we have

$$\inf_{\hat{\Theta}_R} \sup_{\mathcal{D}_{0,R}(t, \beta_R)} \mathcal{R}_R(\hat{\Theta}_R) \asymp \frac{\beta_R t}{\sqrt{n}} \left(\frac{\sigma \sqrt{(t^2 + \sigma^2 p)n}}{t^2} \wedge 1 \right) + \sigma\psi.$$

3 Minimax Optimal and Adaptive Range Estimation

As a direct consequence of our previous results on the extreme column estimation, in this section, we demonstrate that the problem of optimal estimation of the range vector $\mathbf{R}(\Theta) = \Theta_R - \Theta_L$ can be solved in the same manner. Again we consider the normalized ℓ_2 distances $\frac{1}{\sqrt{n}}\|\hat{\mathbf{R}} - \mathbf{R}(\Theta)\|_2$ and denote the corresponding estimation risk as

$$\mathcal{R}_W(\hat{\mathbf{R}}) = \frac{1}{\sqrt{n}}\mathbb{E}\|\hat{\mathbf{R}} - \mathbf{R}(\Theta)\|_2.$$

Similar to our construction of the extreme column estimators, a natural estimator for the range vector can be defined as

$$\hat{\mathbf{R}}^* = \hat{\Theta}_R^* - \hat{\Theta}_L^* = (\hat{v}_{(p)} - \hat{v}_{(1)})X\hat{v}. \quad (3.1)$$

Consequently, similar techniques can be applied to analyze the risk upper bound of $\hat{\mathbf{R}}^*$ as well as the minimax lower bound. Toward this end, we define the parameter space

$$\mathcal{D}_W(t, \beta_R, \beta_L) = \left\{ (\Theta, \pi) \in \mathcal{D} : \begin{array}{l} \text{(A) holds, } \lambda_1 \in [t/8, 8t], \sum_{i=2}^r \lambda_i \leq \sigma\sqrt{\log p}, \\ -\beta_L \leq v_{11} \leq 0 \leq v_{1p} \leq \beta_R, \end{array} \right\}, \quad (3.2)$$

where $t \geq 0$, $p^{-1/2} \leq \beta_R, \beta_L \leq 1$, and define the function $q'(x, y, n, p) = \sigma^2 n \log(np) \left(\frac{1}{x^2} \wedge \frac{1}{y^2} + \frac{1}{\psi} \sqrt{\frac{p}{n \log(pn)}} \right) + \left(\frac{1-x^2}{x^2} \sigma^2 n \psi^2 + \frac{y^2 \sigma^2 p}{1-y^2} \right)$. The following theorem establishes the minimax rate of convergence for estimating $\mathbf{R}(\Theta)$ and the minimax optimality and adaptivity of our proposed estimator $\hat{\mathbf{R}}^*$.

Theorem 3.1 (Minimax Rates). *Let $\beta_W = \beta_R + \beta_L$. Suppose $t^2 \geq c_0 q'(\beta_R \wedge \beta_L, \beta_R \vee \beta_L, n, p)$, $c_1 p^{-1/2} \sqrt{\log p} \leq \{\beta_R, \beta_L\} \leq c_2$ for some constants $c_0, c_1 > 0$ and $0 < c_2 < 1$, and Z has i.i.d. entries $Z_{ij} \sim N(0, \sigma^2)$. Then, for sufficiently large (n, p) ,*

$$\inf_{\hat{\mathbf{R}}} \sup_{\mathcal{D}_W(t, \beta_R, \beta_L)} \mathcal{R}_W(\hat{\mathbf{R}}) \asymp \frac{\beta_W t}{\sqrt{n}} \left(\frac{\sigma \sqrt{(t^2 + \sigma^2 p)n}}{t^2} \wedge 1 \right) + \sigma \psi. \quad (3.3)$$

In particular, the above minimax rates of convergence are simultaneously attained by the estimator $\hat{\mathbf{R}}^$.*

Under the permuted linear growth model, similar arguments about the risk bounds for $\mathcal{R}_W(\hat{\mathbf{R}}^*)$, their interpretations, and the minimax rates of convergence can be obtained.

4 Connections to Other Estimators

4.1 Equivalence to the two-step regression estimator

Ma et al. (2019a) proposed a method to optimally estimate the permutation matrix Π under

the model (1.1). The method is based on a best linear projection that can optimally recover the underlying permutation under both the 0-1 loss and the normalized Kendall's tau distance. Motivated by this study, we consider the following two-step estimator for the extreme values of interest.

To fix ideas, let $\mathbf{r} : \mathbb{R}^p \rightarrow \mathcal{S}_p$ be the ranking operator, which is defined such that for any vector $\mathbf{x} \in \mathbb{R}^p$, $\mathbf{r}(\mathbf{x})$ is the vector of ranks for components of \mathbf{x} in increasing order (whenever there are ties, increasing orders are assigned from left to right). Ma et al. (2019a) defined the best linear projection estimator of π as

$$\hat{\pi} = [\mathbf{r}(\hat{\mathbf{v}})]^{-1}. \quad (4.1)$$

Then, in the first step, we recover/sort the columns of Y to obtain the sorted matrix $\check{Y} = \begin{bmatrix} Y_{\cdot, \hat{\pi}(1)} & Y_{\cdot, \hat{\pi}(2)} & \dots & Y_{\cdot, \hat{\pi}(p)} \end{bmatrix}$. Intuitively, the column-sorted matrix \check{Y} is expected to be close to Θ . In the second step, we fit a simple linear regression between each row of \check{Y} and the sorted projection scores $(\hat{v}_{(1)}, \hat{v}_{(2)}, \dots, \hat{v}_{(p)})$, which characterize the column relative locations. Denote the fitted intercepts as $\boldsymbol{\alpha} = (\alpha_1, \dots, \alpha_n)^\top$ and the slopes as $\boldsymbol{\beta} = (\beta_1, \dots, \beta_n)^\top$. We define the two-step regression estimator of Θ_R , Θ_L and \mathbf{R} as

$$\hat{\Theta}_L^{Reg} = \boldsymbol{\alpha} + \boldsymbol{\beta} \hat{v}_{(1)}, \quad \hat{\Theta}_R^{Reg} = \boldsymbol{\alpha} + \boldsymbol{\beta} \hat{v}_{(p)}, \quad \hat{\mathbf{R}}^{Reg} = \boldsymbol{\beta}(\hat{v}_{(p)} - \hat{v}_{(1)}). \quad (4.2)$$

The following theorem shows that these two-step regression estimators are equivalent to our proposed estimators $\hat{\Theta}_L^*$, $\hat{\Theta}_R^*$ and $\hat{\mathbf{R}}^*$, respectively.

Theorem 4.1. *Under the permuted monotone matrix model (1.1), it holds that*

$$\hat{\Theta}_L^{Reg} = \hat{\Theta}_L^*, \quad \hat{\Theta}_R^{Reg} = \hat{\Theta}_R^*, \quad \hat{\mathbf{R}}^{Reg} = \hat{\mathbf{R}}^*.$$

Therefore, the two-step regression estimators share the same theoretical properties as our proposed estimators such as the minimax optimality and adaptivity. This intrinsic connection between linear regression and approximate rank-one matrix estimation provides another perspective of understanding the optimality of our proposed estimators.

4.2 Sub-optimality of some alternative estimators

To complete our theoretical analysis, we show that the risks of the order statistics (OS) based estimators and the direct sorting (DS) estimators, are uniformly higher than the minimax risk, yielding sub-optimality of these estimators.

Specifically, the DS estimators are defined as $\tilde{\Theta}_R = Y_{\cdot, \hat{\pi}(p)}$, $\tilde{\Theta}_L = Y_{\cdot, \hat{\pi}(1)}$ and $\tilde{\mathbf{R}}_{DS} = Y_{\cdot, \hat{\pi}(p)} - Y_{\cdot, \hat{\pi}(1)}$, where $\hat{\pi}$ is given by (4.1). The OS estimator, as an estimator of the absolute range vector $|\mathbf{R}|$ and closely related to the iRep estimator proposed by Korem et al. (2015), is given by $\tilde{\mathbf{R}}_{OS} = (Y_{i, (p)} - Y_{i, (1)})_{1 \leq i \leq n}$. The following theorem presents the risk lower bounds of these estimators.

Theorem 4.2. Suppose Z has i.i.d. entries $Z_{ij} \sim N(0, \sigma^2)$. Then there exists some constant $C > 0$ such that

$$\inf_{(\Theta, \pi) \in \mathcal{D}} \mathcal{R}_R(\tilde{\Theta}_R) \geq C\sigma, \quad \inf_{(\Theta, \pi) \in \mathcal{D}} \mathcal{R}_W(\tilde{\mathbf{R}}_{DS}) \geq C\sigma.$$

Theorem 4.3. Suppose Z has i.i.d. entries $Z_{ij} \sim N(0, \sigma^2)$ and $|\mathbf{R}| = \mathbf{R}$. Then there exists some constant $C > 0$ such that

$$\inf_{(\Theta, \pi) \in \mathcal{D}} \mathcal{R}_W(\tilde{\mathbf{R}}_{OS}) \geq C\sigma.$$

Theorem 4.2 shows that, although one can optimally recover the underlying permutation, directly using the sorted observations to estimate the corresponding extreme columns is sub-optimal. In line with the arguments made in Section 2.2, Theorem 4.3 shows that, a good estimator of the extreme values should combine the information across samples rather than estimate each coordinate individually. This theorem along with our previous results makes a compelling example concerning compound decision problems, showing the admissibility of the compound rules as well as the asymptotic subminimaxity of the simple rules (Robbins, 1951, 1964).

5 Numerical Studies

5.1 Simulation with model-generated data

To demonstrate our theoretical results and to compare with alternative and existing methods, we generate data from model (1.1) with various configurations of the signal matrix Θ . Specifically, the signal matrix $\Theta = (\theta_{ij}) \in \mathbb{R}^{n \times p}$ is generated under the following two regimes:

- $S_1(n, p, \alpha)$: For any $1 \leq i \leq n$, $\theta_{ij} = a_i \eta_j + b_i$ for $1 \leq j \leq p$, where $a_i \sim \text{Unif}(0, \alpha)$, $b_i \sim \text{Unif}(0, 6)$ and $(\eta_1, \dots, \eta_p) = (-1, 0, 0, \dots, 0, 1)$;
- $S_2(n, p, \alpha)$: For any $1 \leq i \leq n$, $\theta_{ij} = \log(1 + a_i j + \beta_i)$ for $1 \leq j \leq p$ where $a_i \sim \text{Unif}(0, \alpha)$ and $b_i \sim \text{Unif}(0, 6)$.

By construction, $S_1(\alpha, n, p)$ belongs to the linear growth model whereas $S_2(\alpha, n, p)$ does not. The elements of Z are drawn from i.i.d. standard normal distributions, and, without loss of generality, we set $\Pi = \mathbf{I}_p$.

For the extreme column Θ_R , we compare the empirical performance of our proposed estimator $\hat{\Theta}_R^*$ with (i) the direct sorting estimator (DS) $\tilde{\Theta}_R$ defined in Section 4.2, and (ii) the order statistic estimator (OS) $\check{\Theta}_R = (Y_{i,(p)})_{1 \leq i \leq n}$, as all the rows of Θ are monotonic increasing. For the range vector $\mathbf{R}(\Theta)$, we compare our proposed estimator $\hat{\mathbf{R}}^*$ with (i) the direct sorting estimator (DS) $\tilde{\mathbf{R}}_{DS}$ and (ii) the order statistic estimator (OS) $\tilde{\mathbf{R}}_{OS}$, both defined in Section 4.2. We use the empirical risk (averaged normalized ℓ_2 distance) to compare these methods. For each setting, we evaluate the empirical performance of each method over a range of n , p and α . Each setting is repeated for 200 times.

The results are summarized as boxplots in Figure 2 and Figure 3. The empirical results agree with our theory in the following perspectives: (i) our proposed estimators $\hat{\Theta}_R^*$ and $\hat{\mathbf{R}}^*$ perform the best in all the settings; (ii) in the middle two plots of Figure 2 and 3, the risks of our proposed estimators decrease as n grows, which also agrees with our theorems. In addition, in the top left panel of Figure 2 and 3 we observe that the risks of the OS estimator decrease as α increases. This is because under $S_1(\alpha, p, n)$, the parameter α characterizes the separateness of the two extreme columns from the other columns. The OS estimators would apparently favour the cases where the separation is significant. In general, the DS estimators outperform the OS estimators, again showing the advantage of the compound estimators.

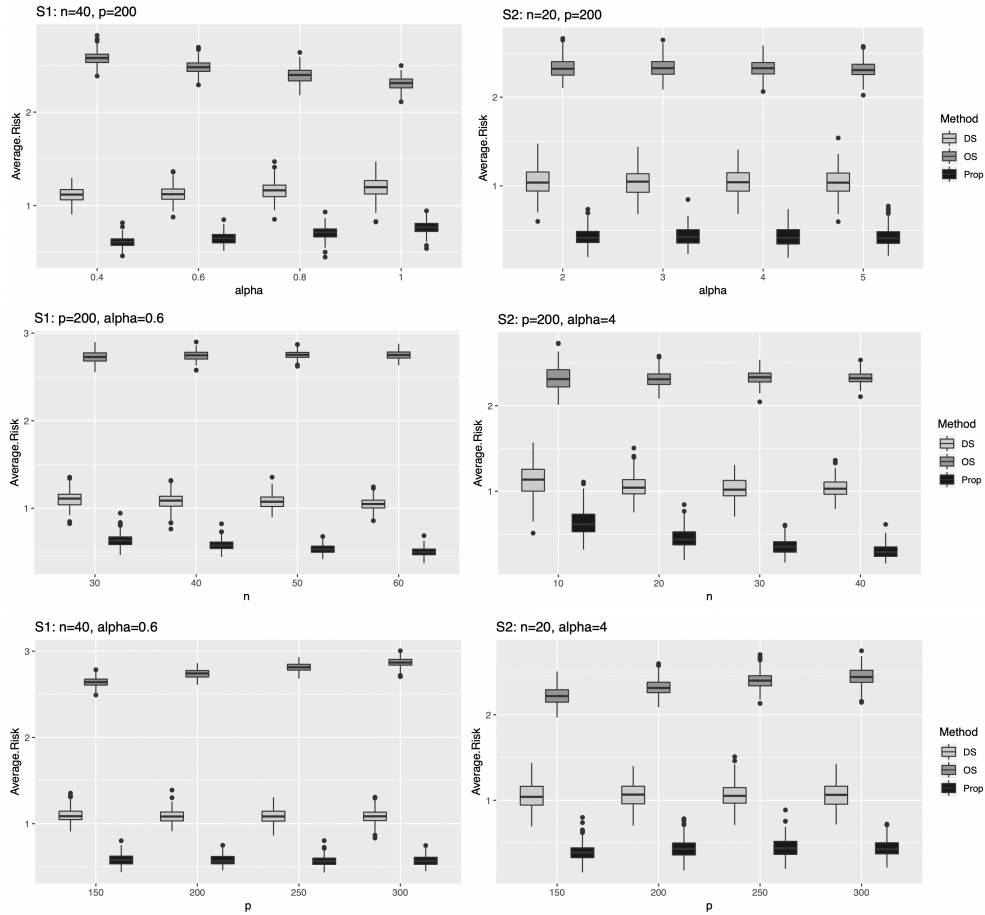


Figure 2: Boxplots of the empirical risks for the estimators of Θ_R under two different models, $S_1(\alpha, p, n)$ and $S_2(\alpha, p, n)$. DS: the direct sorting estimator $\tilde{\Theta}_R$ defined in Section 4.2; OS: the order statistic estimator $\tilde{\Theta}_R = (Y_{i,(p)})_{1 \leq i \leq n}$; Prop: proposed estimator $\hat{\Theta}_R^*$.

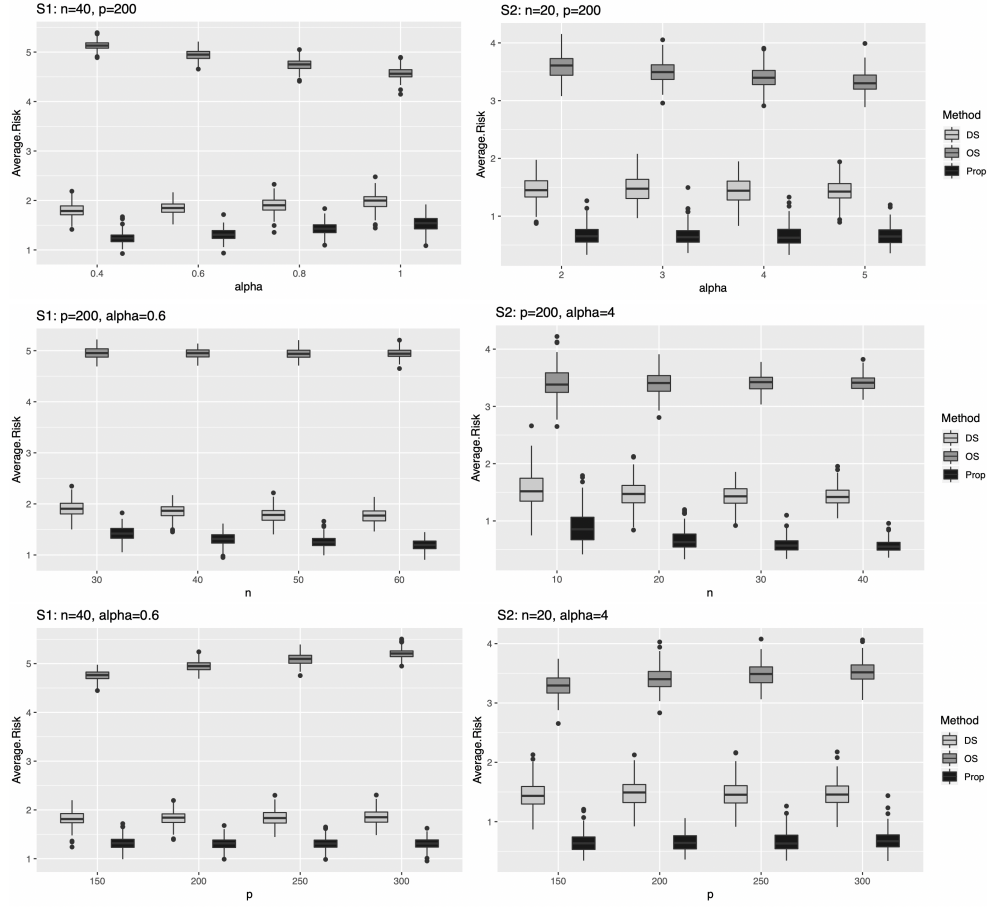


Figure 3: Boxplots of the empirical risks for the estimators of \mathbf{R} under two different models, $S_1(\alpha, p, n)$ and $S_2(\alpha, p, n)$. DS: the direct sorting estimator $\hat{\mathbf{R}}_{DS}$ defined in Section 4.2; OS: the order statistic estimator $\hat{\mathbf{R}}_{OS}$ defined in Section 4.2; Prop: proposed estimator $\hat{\mathbf{R}}^*$.

5.2 Simulation with synthetic microbiome metagenomic data

We then evaluate the empirical performance of our proposed method using a synthetic metagenomic sequencing dataset (Gao and Li, 2018) by generating sequencing reads based on 45 closely related bacterial genomes in 50 independent samples. Particularly, Gao and Li (2018) presented a synthetic shotgun metagenomic sequencing dataset of a community of 45 phylogenetically related species from 15 genera of five different phyla with known RefSeq ID, taxonomy and replication origin (Gao et al., 2013). To generate the metagenomic reads, reference genome sequences of randomly selected three species in each genus were downloaded from NCBI. Read coverages were generated along the genome based on an exponential distribution with a specified peak-to-trough ratio and a function of accumulative distribution of read coverages along the genome was calculated. Sequencing reads were then generated using the above accumulative distribution functions and a random location for each read on the genome, until the total read number achieved a randomly assigned average coverage

between 0.5 and 10 folds for the species in a sample. Sequencing errors including substitution, insertion and deletion were simulated in a position- and nucleotide-specific pattern according to the metagenomic sequencing error profile of Illumina.

For the final data set, the average nucleotide identities (ANI) between species within each genus ranged from 66.6% to 91.2%. The probability of one species existing in each of the 50 simulated samples was set as 0.6, and a total of 1,336 average coverages and the corresponding PTRs were randomly and independently assigned. After the same processing, filtering, and CG-adjustment steps as in Gao and Li (2018), the final data set included genome assemblies of 41 species. For each species, we obtained the permuted matrix of log-contig coverage with the number of samples ranging from 29 to 46 and the number of contigs from 47 to 482.

Similar to Gao and Li (2018), we provide estimates of the log-PTRs of the assembled species for all the samples, defined as \mathbf{R} , using our previous notations. As a comparison, in addition to our proposed method ($\hat{\mathbf{R}}^*$), we also considered the iRep estimator proposed in Brown et al. (2016), where the contigs of a given species were ordered for each sample separately based on the read counts observed, before fitting a piece-wise linear regression function. We evaluate these methods by considering the ℓ_2 distance between the vectors of the estimated and the true log-PTRs. To generalize our evaluation to diverse metagenomic datasets, we also evaluate the effect of sample size as well as contig numbers by randomly selecting subsets of samples or contigs from each dataset. The selection was made with replacement.

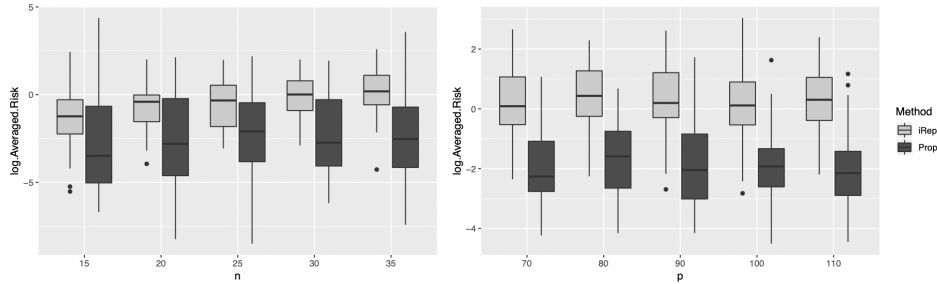


Figure 4: Boxplots of the ℓ_2 distance between the vectors of the estimated and the true log-PTRs for different sample sizes n and different numbers of contigs p . The darker ones correspond to our proposed method and the lighter ones correspond to the iRep estimation method.

The results are summarized in Figure 4. As n or p varies, our proposed estimator performs consistently better than iRep. Moreover, the performance of our proposed method is not sensitive to the sample size, the number of contigs from the genome assemblies or the underlying true PTRs. These results partially explain why the DEMIC algorithm has superior performance compared to the existing ones (Gao and Li, 2018).

Table 1: Analysis of bacterial growth rates among CD, UC and non-IBD samples. Bins that show significantly different growth rates and their taxonomic annotations are presented. (n_1, n_2, n_3) : numbers of samples of CD, UC and non-IBD samples that carried the respective bin (assembled bacterial genome).

Bins	(n_1, n_2, n_3)	P-values	Taxonomic Annotations
bin.054	(54,32,54)	0.015	Roseburia (genus)
bin.090	(38,41,52)	0.005	Faecalibacterium (genus)
bin.091	(26,40,52)	0.016	Clostridiales (order)
bin.099	(30,32,49)	< 0.001	Subdoligranulum (genus)
bin.465	(36,41,33)	0.043	Dialister (genus)

5.3 Analysis of a real microbiome metagenomic data set

We complete our numerical study by analyzing a metagenomic dataset from the NIH Integrative Human Microbiome Project (iHMP). As part of the iHMP, the Inflammatory Bowel Disease (IBD) Multi’omics project is a multi-institutional effort to investigate the differences in gut microbiome communities among adults and children with IBD (Lloyd-Price et al., 2019) and normal non-IBD controls. Many studies have reported strong associations between IBD, including both Crohn’s disease (CD) and ulcerative colitis (UC) and gut microbiota composition. In contrast, we focus on comparing the bacterial growth rates between UC, CD and normal non-IBD individuals using the methods proposed.

The metagenomic datasets, which include 300 samples of the CD, UC and non-IBD subjects, were downloaded from the IBDMDB website (<https://www.ibdmdb.org>). Specifically, we randomly select 100 samples of UC, CD and normal non-IBD samples, respectively. For each sample. the sequencing data was obtained from the stool sample using Illumina shotgun sequencing. We first apply MEGAHIT (Li et al., 2015) (version 1.1.1) to perform metagenomic co-assembly. The co-assembled contigs were then clustered into metagenomic bins (genome assemblies) using MaxBin (Wu et al., 2015) version 2.2.4. Finally, Bowtie 2 (Langmead and Salzberg, 2012) (version 2.3.2) was used to align reads back to the assembled contigs for each of the samples. The output alignment results were then sorted by samtools (Li et al., 2009) (0.1.19).

After these preparations, the DEMIC algorithm was applied to obtain estimates the PTRs (ePTRs) of a given species represented by a contig cluster (bin) for each sample. As a result, ePTRs of 25 bins were obtained for subsets of the UC (n_1), CD (n_2) and non-IBD (n_3) samples with $n_1 + n_2 + n_3 \geq 100$, as some contig clusters may not be carried or abundant enough in some samples. For each bin, we compare the ePTRs among the UC, CD and non-IBD samples using an F-test. We applied the CAT/BAT algorithm (von Meijenfildt et al., 2019) that compares the metagenomic assembled bins to a taxonomy database to obtain the taxonomic annotations of the 25 bins.

Interestingly, based on the F-test, among the 25 contig clusters, 5 of them show significant

Table 2: p-values from pairwise t -tests of differential growth rates between different groups for five genome assembly bins.

Bins	UC vs. CD	UC vs. non-IBD	CD vs. non-IBD
bin.054	0.525	0.004	0.081
bin.090	0.392	0.016	0.004
bin.091	0.012	0.054	0.335
bin.099	0.960	< 0.001	< 0.001
bin.465	0.042	0.818	0.026

difference in ePTRs among the UC, CD and non-IBD samples (Table 1). Due to page limitation, in Table 1 we only provide the taxonomic annotation of the bins in terms of their genus – except for bin.091 which can only be determined up to orders (see our Supplementary Material for the complete annotations). We then performed pairwise comparisons using two-sample t -test for the 5 differential bins (Table 2). We found that the difference in the growth rates of bin.054 (Roseburia), bin.090 (Faecalibacterium) and bin.099 (Subdoligranulum) are more significant between IBD and non-IBD samples. In particular, boxplots in our Supplementary Material indicate higher growth rates of bin.054 (Roseburia) and bin.090 (Faecalibacterium), and a lower growth rates of bin.099 (Subdoligranulum) for IBD samples when compared to the non-IBD samples. Moreover, the growth rates of bin.091 (Clostridiales) is significantly higher among UC samples, whereas the growth rate of bin.465 (Dialister) is significantly higher among the CD samples, comparing to the samples of the other two categories. These results show that CD and UC patients or IBD and non-IBD patients differed not only in relative abundance of certain bacteria, they also differed in growth rates for certain bacteria, an important insight from our analysis.

6 Discussion

In this paper, we consider the permuted monotone matrix where the noise matrix Z is assumed to have *i.i.d.* entries following the Gaussian distribution. However, we emphasize that the Gaussian assumption is not essential in the proofs of risk upper bounds. The results can be easily generalized to the cases where the entries of Z are independent centered sub-Gaussian random variables with parameter σ^2 . In the presence of heteroskedastic noises, such as (i) the columns of the noise matrix are not independent, or (ii) the variances of the noise matrix entries are not identical, we argue that, as long as the marginal distributions of the noise matrix remain sub-Gaussian, the analytical framework of our paper can still be applied. This is related to some recent work of Zhang et al. (2018), where the problem of PCA and SVD with heteroskedastic noise is studied. In particular, the key analytical tools, including the concentration/perturbation bounds associated to the low-rank matrix denoising models with heteroskedastic noise, parallel to those applied in the current work can be derived by generalizing the results of Zhang et al. (2018). However, such extensions

are non-trivial and we plan to pursue this direction in a follow-up study.

Moreover, under our current analytical framework that is built upon the leading singular vector property demonstrated in Section 2.1, we focus on approximately rank-one signal matrices. As a result, it remains an open question whether there exists an adaptive optimal estimator over the general unrestricted parameter space. The results of our current work have shown the power of first order approximation via the first spectral triple $(\lambda_1, \mathbf{u}_1, \mathbf{v}_1)$. However, it is interesting to investigate whether including more leading singular values/vectors would be helpful in estimating the extreme columns associated with the permuted matrix.

7 Proofs

For reasons of space, we prove Theorems 2.3 and 4.1 in detail. The proofs of other theorems and the technical results are given in Ma et al. (2019b).

Proof of Theorem 2.3. The proof of this theorem relies on the following key proposition concerning four important lower bounds over some specially designed parameter spaces.

Proposition 7.1. *Suppose Z has i.i.d. entries $Z_{ij} \sim N(0, \sigma^2)$. Then*

(i) *for any $p \geq 8$, $t^2 \geq \frac{1-\beta_R^2/2}{\beta_R^2-4/p} \sigma^2 \log p$ and $p^{-1/2} \sqrt{\log p} \leq \beta_R \leq 1$,*

$$\inf_{\hat{\Theta}_R} \sup_{\mathcal{D}_R(t, \beta_R)} \mathbb{E} \|\hat{\Theta}_R - \Theta_R\|_2 \gtrsim \sigma \sqrt{\log p}; \quad (7.1)$$

(ii) *for any $p \geq 8$, $t^2 \geq \frac{\sigma^2 n}{p} \frac{2-3\beta_R^2}{\beta_R^2}$ and $p^{-1/2} \leq \beta_R \leq 1$,*

$$\inf_{\hat{\Theta}_R} \sup_{\mathcal{D}_R(t, \beta_R)} \mathbb{E} \|\hat{\Theta}_R - \Theta_R\|_2 \gtrsim \sigma \sqrt{\frac{n}{p}}, \quad (7.2)$$

$$\inf_{\hat{\Theta}_R} \sup_{\mathcal{D}_R(t, \beta_R)} \mathbb{E} \|\hat{\Theta}_R - \Theta_R\|_2 \gtrsim t \beta_R \left(1 \wedge \frac{\sigma \sqrt{n}}{t} \right); \quad (7.3)$$

(iii) *for any $c_1 p^{-1/2} \sqrt{\log p} \leq \beta_R \leq c_2 < 1$ and $\frac{\beta_R^2 \sigma^2 p}{1-\beta_R^2} \leq t^2 \leq \sigma^2 p/4$,*

$$\inf_{\hat{\Theta}_R} \sup_{\mathcal{D}_R(t, \beta_R)} \mathbb{E} \|\hat{\Theta}_R - \Theta_R\|_2 \gtrsim t \beta_R \left(1 \wedge \frac{\sigma \sqrt{n(t^2 + \sigma^2 p)}}{t^2} \right); \quad (7.4)$$

For any pair (t, β_R) satisfying the condition of Theorem 2.3, by Proposition 7.1 (i), we have $\inf_{\hat{\Theta}_R} \sup_{\mathcal{D}_R(t, \beta_R)} \mathbb{E} \|\hat{\Theta}_R - \Theta_R\|_2 \gtrsim \sigma \sqrt{\log p}$. Along with (7.2) of Proposition 7.1 (ii), we have

$$\inf_{\hat{\Theta}_R} \sup_{\mathcal{D}_R(t, \beta_R)} \mathbb{E} \|\hat{\Theta}_R - \Theta_R\|_2 \gtrsim \sigma \sqrt{n} \psi(n, p). \quad (7.5)$$

It remains to prove

$$\inf_{\hat{\Theta}_R} \sup_{\mathcal{D}_R(t, \beta_R)} \mathbb{E} \|\hat{\Theta}_R - \Theta_R\|_2 \gtrsim t \beta_R \left(1 \wedge \frac{\sigma \sqrt{n(t^2 + \sigma^2 p)}}{t^2} \right). \quad (7.6)$$

If $t^2 \geq \sigma^2 p/4$, we have $\sigma \sqrt{n}/t \gtrsim \sigma \sqrt{n(t^2 + \sigma^2 p)}/t^2$, so that (7.6) holds by (7.3). If $t^2 \leq \sigma^2 p/4$, Proposition 7.1 (iii) applies directly. \square

Proof of Proposition 7.1. To establish sharp minimax lower bounds, we consider subsets of \mathcal{D} whose geometric features best describe the essential difficulties for estimating Θ_R .

Proof of (7.1). The proof relies on our general lower bound for testing two composite hypotheses about some high-dimensional operator (Lemma 2.1). We define the one-element set

$$\mathcal{H}_0(\eta) = \{(\Theta, \pi) = (\mathbf{e}_1 \boldsymbol{\eta}^\top, id)\},$$

where $\mathbf{e}_1 = (1, 0, 0, \dots, 0)^\top \in \mathbb{R}^n$ and $\boldsymbol{\eta} \in \mathbb{R}^p$ is defined such that, for some $\eta > 0$ to be determined later, the first $k = \lfloor p/2 \rfloor$ coordinates of $\boldsymbol{\eta}$ are $-(\eta, \dots, \eta)$, the last k coordinates of $\boldsymbol{\eta}$ are (η, \dots, η) , and set the $(\lfloor p/2 \rfloor + 1)$ -th coordinate of $\boldsymbol{\eta}$ as 0 if p is odd. In addition, we define the set

$$\mathcal{H}_1(\eta) = \{(\Theta, \pi) : \Theta = \mathbf{e}_1 \boldsymbol{\eta}'^\top, \pi \in T\},$$

where $\boldsymbol{\eta}' = \boldsymbol{\eta} + \frac{\sigma}{2} \sqrt{\log p} \cdot (-1, 0, \dots, 0, 1)^\top$, and $T = \{\pi \in \mathcal{S}_p : \pi \text{ is a transposition between } k\text{-th and } p\text{-th element, } \forall \lfloor p/2 \rfloor + 1 \leq k \leq p\}$. For any pair (t, β_R) satisfying the condition of Proposition 7.1 (i), to find specific η such that $\mathcal{H}_0(\eta) \subset \mathcal{D}_R(t, \beta_R)$ and $\mathcal{H}_1(\eta) \subset \mathcal{D}_R(t, \beta_R)$, we consider η such that

$$t = \|\mathbf{e}_1\|_2 \|\boldsymbol{\eta}\|_2 = \sqrt{p\eta^2}, \quad \beta_R^2 \geq \frac{2(\eta + \frac{\sigma}{2} \sqrt{\log p})^2}{\|\boldsymbol{\eta}'\|_2^2} \geq \frac{\eta^2}{\|\boldsymbol{\eta}\|_2^2}, \quad (7.7)$$

where the last inequality holds by construction. Note that the second equation holds if

$$\beta_R^2 \geq \frac{4\eta^2 + \sigma^2 \log p}{p\eta^2 + \frac{\sigma^2}{2} \log p} \quad \text{or} \quad \eta^2 \geq \frac{1 - \beta_R^2/2}{p\beta_R^2 - 4} \cdot \sigma^2 \log p.$$

Plug this into the first equation of (7.7), we have

$$t^2 = p\eta^2 \geq \frac{1 - \beta_R^2/2}{\beta_R^2 - 4p^{-1}} \cdot \sigma^2 \log p.$$

Hence, as long as $t^2 \geq \frac{1-\beta_R^2/2}{\beta_R^2-4/p} \sigma^2 \log p$, we can always find η such that $\mathcal{H}_0(\eta)$. On the other hand, it can be checked that for any $(\Theta, \pi) \in \mathcal{H}_1(\eta)$,

$$t^2 \leq p\eta^2 + \frac{\sigma^2}{2} \log p \leq \|\Theta\|^2 \leq (p+2)\eta^2 + \sigma^2 \log p \leq 4t^2,$$

so that $\mathcal{H}_1(\eta) \subset \mathcal{D}_R(t, \beta_R)$.

Intuitively, the construction of \mathcal{H}_0 and \mathcal{H}_1 reflects the effects of perturbing the extreme values of the first right singular vector of Θ . The subset \mathcal{H}_1 is constructed so that a mixture distribution based on parameters uniformly chosen from \mathcal{H}_1 will be statistically indistinguishable from the null distribution defined on \mathcal{H}_0 . Toward this end, we define μ_1 as the uniform prior over $\mathcal{H}_1(\eta)$, and define μ_0 as the point-mass at the one-point set $\mathcal{H}_0(\eta)$. Let $F : \mathcal{D} \rightarrow \mathbb{R}^n$ be the function such that $F(\Theta)$ is the rightmost column Θ_R of Θ . It holds that

$$\mu_0((\Theta, \mu) \in \mathcal{D} : F(\Theta) = (\eta, 0, \dots, 0)^\top \in \mathbb{R}^n) = 1,$$

$$\mu_1((\Theta, \pi) \in \mathcal{D} : F(\Theta) = (\eta + \frac{\sigma}{2} \sqrt{\log p}, 0, \dots, 0)^\top \in \mathbb{R}^n) = 1.$$

Then $\|F(\Theta_0) - F(\Theta_1)\|_2 = \frac{\sigma}{2} \sqrt{\log p}$ for any $\Theta_0 \in \mathcal{H}_0$ and $\Theta_1 \in \mathcal{H}_1$. Moreover, let P_0 and P_1 be the posterior distributions of $Y = \Theta\Pi + Z$. The following lemma controls the chi-square divergence $\chi^2(P_1, P_0)$.

Lemma 7.1. *Under the condition of Proposition 7.1 (i), it holds that $\chi^2(P_1, P_0) \leq 3$.*

Lemmas 2.1 and 7.1 yield

$$\inf_{\hat{\Theta}} \sup_{\mathcal{D}_R(t, \beta_R)} P\left(\|\hat{\Theta} - \Theta_R\|_2 \geq \frac{\sigma}{4} \sqrt{\log p}\right) \geq 0.01.$$

The final result then follows from the Markov's inequality.

Proof of (7.2). The proof of this lower bound relies on the following general lower bound for testing multiple hypotheses.

Lemma 7.2 (Tsybakov 2009). *Assume that $M \geq 2$ and suppose that Θ contains elements $\theta_0, \theta_1, \dots, \theta_M$ such that: (i) $d(\theta_j, \theta_k) \geq 2s > 0$ for any $0 \leq j < k \leq M$; (ii) it holds that $\frac{1}{M} \sum_{j=1}^M D(P_j, P_0) \leq \alpha \log M$ with $0 < \alpha < 1/8$ and $P_j = P_{\theta_j}$ for $j = 0, 1, \dots, M$. Then*

$$\inf_{\hat{\theta}} \sup_{\theta \in \Theta} P_{\theta}(d(\hat{\theta}, \theta) \geq s) \geq \frac{\sqrt{M}}{1 + \sqrt{M}} \left(1 - 2\alpha - \sqrt{\frac{2\alpha}{\log M}}\right) > 0.$$

Let $\mathbf{v} = (-p^{-1/2}, -\delta, \dots, \delta, p^{-1/2}) \in \mathbb{R}^p$ for some $0 < \delta \leq p^{-1/2}$. We consider the pairs (Θ, id) such that $\pi = id$ and $\Theta = \beta \mathbf{v}^\top$ where $\beta \in \{\sigma\xi, \sigma\xi(1 + \rho)\}^n$ for some $\xi, \rho > 0$. By the following

Varshamov-Gilbert bound (Lemma 4.7 in Massart (2007)), define a discrete parameter space

$$\mathcal{D}_M(\rho, \delta, \xi) = \{(\Theta, \pi) = (\beta \mathbf{v}^\top, id) : \beta \in \mathcal{T}(\rho, \xi)\},$$

where $\mathcal{T}(\rho, \xi)$ consists of $\beta \in \{\sigma\xi, \sigma\xi(1+\rho)\}^n$ such that (i) the vector $\beta^{(0)} = (\sigma\xi, \dots, \sigma\xi) \in \mathcal{T}(\rho, \xi)$, (ii) for any $\beta^{(i)}$ and $\beta^{(j)}$ from $\mathcal{T}(\rho, \xi)$, it holds that $\|\beta^{(i)} - \beta^{(j)}\|_0 \geq n/8$, and (iii) $\log |\mathcal{T}(\rho, \xi)| \geq 0.08n$. Intuitively, the set $\mathcal{D}_M(\rho, \delta, \xi)$ makes a local packing of the parameter space \mathcal{D} , which emphasizes the effect of perturbing the first left singular vector of Θ .

Lemma 7.3 (Varshamov-Gilbert Bound). *Let $\Omega = \{0, 1\}^n$ and $n \geq 8$. Then there exists a subset $\{\omega^{(0)}, \dots, \omega^{(M)}\}$ of Ω such that $\omega^{(0)} = (0, \dots, 0)$ and $\|\omega^{(j)} - \omega^{(k)}\|_0 \geq \frac{n}{8}$ for $0 \leq j < k \leq M$, and $M \geq 2^{n/8}$.*

From the above construction, one can check immediately that for any $\Theta^{(i)} = \beta^{(i)} \mathbf{v}^\top$ and $\Theta^{(j)} = \beta^{(j)} \mathbf{v}^\top$ from \mathcal{D}_M , it holds that

$$\|F(\Theta^{(i)}) - F(\Theta^{(j)})\|_2 = \frac{\|\beta^{(i)} - \beta^{(j)}\|_2}{\sqrt{p}} \geq \frac{\sigma\xi\rho}{\sqrt{p}} \sqrt{\frac{n}{8}}.$$

Let P_k be the probability measure of Y corresponding to $\Theta^{(k)} = \beta^{(k)} \mathbf{v}^\top$. We have the KL-divergence

$$D(P_k \| P_0) = \frac{1}{2\sigma^2} \|\beta^{(k)} \mathbf{v}^\top - \beta^{(0)} \mathbf{v}^\top\|_F^2 \lesssim \frac{n\xi^2\rho^2}{2} \left(\frac{1}{p} + p\delta^2 \right). \quad (7.8)$$

If we choose (ξ, ρ, δ) such that for some sufficiently large constants $C_1, C_2 > 0$

$$C_1^{-1} \leq \xi^2\rho^2 \leq C_2^{-1}(1/p + p\delta^2)^{-1}, \quad (7.9)$$

then it holds that $D(P_k \| P_0) < \frac{1}{8} \log |\mathcal{D}_M|$ and by Lemma 7.2,

$$\inf_{\hat{\Theta}} \sup_{\mathcal{D}_M} P(\|\hat{\Theta} - \Theta_R\|_2 \geq C\sigma\sqrt{n/p}) \geq c. \quad (7.10)$$

Now, to obtain (7.2), it suffices to show that, for any (t, β_R) satisfying the conditions of Proposition 7.1 (ii), we can find (ρ, δ, ξ) such that (7.9) holds and $\mathcal{D}_M(\rho, \delta, \xi) \subseteq \mathcal{D}_R(t, \beta_R)$. Towards this end, for any above (t, β_R) , we choose $\delta^2 = \max(0, \frac{1-2\beta_R^2}{p(p-2)\beta_R^2})$. Now if $C_2 t^2 \geq \sigma^2 n$, we set

$$\rho^2 = \frac{\sigma^2 n}{C_2 t^2} \leq 1, \quad \xi^2 = (1/p + p\delta^2)^{-1} \cdot \frac{t^2}{\sigma^2 n};$$

if $C_2 t^2 < \sigma^2 n$, we set

$$\xi^2 = \frac{t^2}{\sigma^2 n}, \quad \rho^2 = (1/p + p\delta^2)^{-1}.$$

Note that $(1/p + p\delta^2)^{-1} > 1$ and by $t^2 \geq \frac{\sigma^2 n}{p} \frac{2-3\beta_R^2}{\beta_R^2}$ it holds that $(1/p + p\delta^2)^{-1} > \sigma^2 n/t^2$. Under either cases, (δ, ξ, ρ) satisfies (7.9). In particular, for any $(\Theta, \pi) \in \mathcal{D}_M(\rho, \delta, \xi)$,

$$\frac{t^2}{8} \leq n\sigma^2\xi^2(2/p + (p-2)\delta^2) \leq \|\Theta\|^2 \leq n(1+\rho)^2\sigma^2\xi^2(2/p + (p-2)\delta^2) \leq 8t^2,$$

for all $p \geq 8$, and the largest component of the first right singular vector of Θ is bounded by β_R . Therefore, $\mathcal{D}_M(\rho, \delta, \xi) \subseteq \mathcal{D}_R(t, \beta_R)$. Consequently,

$$\inf_{\hat{\Theta}} \sup_{\mathcal{D}_R(t, \beta_R)} P(\|\hat{\Theta} - \Theta_R\|_2 \geq C\sigma\sqrt{n/p}) \geq c \quad (7.11)$$

for some absolute constants $C, c > 0$. The lower bound (7.2) then follows from the Markov inequality.

Proof of (7.3). Similar to the proof of (7.2), the lower bound (7.3) is again obtained by applying Lemma 7.2 and considering some subset $\mathcal{D}_m \subset \mathcal{D}(t, \beta_R)$ for any (t, β_R) satisfying the condition of Proposition 7.1 (ii). Specifically, for some fixed unit vector $\mathbf{v}_0 = (v_1, \dots, v_p)^\top \in \mathbb{R}^p$ where $v_1 \leq v_2 \leq \dots \leq v_p = \beta_R$ and $\sum_{j=1}^p v_j = 0$, we define

$$\mathcal{D}_{\mathbf{v}_0} = \{(\Theta_{\mathbf{u}}, id) \in \mathcal{D}_R(t, \beta_R) : \Theta_{\mathbf{u}} = t\mathbf{u}\mathbf{v}_0^\top, \|\mathbf{u}\|_2 = 1\}.$$

For any $(\Theta_{\mathbf{u}}, id) \in \mathcal{D}_{\mathbf{v}_0}$, let $P_{\mathbf{u}}$ be the probability measure of $Y = \Theta_{\mathbf{u}} + Z \in \mathbb{R}^{n \times p}$ with $Z_{ij} \sim N(0, \sigma^2)$. Then the KL-divergence satisfies

$$D(P_{\mathbf{u}} \| P_{\mathbf{u}'}) = \frac{1}{2\sigma^2} \|t\mathbf{u}\mathbf{v}_0^\top - t\mathbf{u}'\mathbf{v}_0^\top\|_F^2 = \frac{t^2}{2\sigma^2} \|\mathbf{u} - \mathbf{u}'\|_2^2.$$

Now for any fixed unit vector $\mathbf{u}_0 \in \mathbb{R}^n$, we consider the ball with radius $0 < \epsilon < 1$ and centered at \mathbf{u}_0

$$B(\mathbf{u}_0, \epsilon) = \{\mathbf{u} \in \mathbb{R}^n : \|\mathbf{u}\|_2 = 1, \sqrt{1 - (\mathbf{u}_0^\top \mathbf{u})^2} \leq \epsilon\}$$

Since $\sqrt{1 - (\mathbf{u}^\top \mathbf{u}')^2} = \|\mathbf{u}\mathbf{u}^\top - \mathbf{u}'\mathbf{u}'^\top\|_F / \sqrt{2}$, to construct a local packing of $B(\mathbf{u}_0, \epsilon)$, we can use the following lemma regarding the metric entropy of the Grassmannian manifold $G(k, r)$ from Cai et al. (2013) (see also Proposition 8 of Szarek (1982).)

Lemma 7.4 (Cai et al. 2013). *For any $V \in O(k, r)$, identifying the subspace $\text{span}(V)$ with its projection matrix VV^\top , define the metric on the Grassmannian manifold $G(k, r)$ by $\rho(VV^\top, UU^\top) = \|VV^\top - UU^\top\|_F$. Then for any $\epsilon \in (0, \sqrt{2(r \wedge (k-r))})$,*

$$\left(\frac{c_0}{\epsilon}\right)^{r(k-r)} \leq \mathcal{N}(G(k, r), \epsilon) \leq \left(\frac{c_1}{\epsilon}\right)^{r(k-r)},$$

where $\mathcal{N}(E, \epsilon)$ is the ϵ -covering number of E and c_0, c_1 are absolute constants. Moreover, for any $V \in \mathcal{O}(k, r)$ and any $\alpha \in (0, 1)$, $\mathcal{M}(B(V, \epsilon), \alpha\epsilon) \geq \left(\frac{c_0}{\alpha c_1}\right)^{r(k-r)}$, where $\mathcal{M}(E, \epsilon)$ is the ϵ -packing number of E .

As a result, for any $\alpha, \epsilon \in (0, 1)$, there exist $\mathbf{u}_1, \dots, \mathbf{u}_m \in B(\mathbf{u}_0, \epsilon)$, such that $m \geq (c/\alpha)^{n-1}$ and $\min_{1 \leq i \neq j \leq m} \sqrt{1 - (\mathbf{u}_i^\top \mathbf{u}_j)^2} \geq \alpha\epsilon$. Without loss of generality, we choose $\mathbf{u}_1, \dots, \mathbf{u}_m$ such that $\mathbf{u}_i^\top \mathbf{u}_j \geq 0$ for all $i, j \in \{1, \dots, m\}$ (this can be done if $\epsilon^2 < 0.5$). Hence, by focusing on the m point subset $\mathcal{D}_m = \{(\Theta_{\mathbf{u}}, id) \in \mathcal{D}_{\mathbf{v}_0} : \mathbf{u} \in \{\mathbf{u}_1, \dots, \mathbf{u}_m\}\}$, for any $1 \leq i \neq j \leq m$,

$$\begin{aligned} \|F(\Theta_{\mathbf{u}_i}) - F(\Theta_{\mathbf{u}_j})\|_2 &= \|t\mathbf{u}_i\beta_R - t\mathbf{u}_j\beta_R\|_2 \geq t\beta_R\sqrt{2(1 - \mathbf{u}_i^\top \mathbf{u}_j)} \\ &= t\beta_R\sqrt{\frac{2(1 - (\mathbf{u}_i^\top \mathbf{u}_j)^2)}{(1 + \mathbf{u}_i^\top \mathbf{u}_j)}} \geq t\beta_R\sqrt{1 - (\mathbf{u}_i^\top \mathbf{u}_j)^2} \geq t\beta_R\alpha\epsilon \end{aligned}$$

and the KL-divergence $\max_{1 \leq i \leq m} D(P_{\mathbf{u}_i} \| P_{\mathbf{u}_0}) = \frac{t^2}{2\sigma^2} \|\mathbf{u}_i - \mathbf{u}_0\|_2^2 \leq t^2\epsilon^2/\sigma^2$. If we set $\epsilon^2 = c(\sigma^2 n/t^2 \wedge 1)$ for some constant $c > 0$, we have

$$\max_{1 \leq i \leq m} D(P_{\mathbf{u}_i} \| P_{\mathbf{u}_0}) \leq \frac{ct^2}{\sigma^2} \left(\frac{\sigma^2 n}{t^2} \wedge 1 \right) \leq \log m.$$

Then Lemma 7.2 yields

$$\inf_{\hat{\Theta}} \sup_{\mathcal{D}_m} P\left(\|\hat{\Theta} - \Theta_R\|_2 \geq ct\beta_R\epsilon\right) \geq C$$

for some constants $C, c > 0$. Thus, the desired lower bound follows from the Markov inequality and the inclusion $\mathcal{D}_m \subset \mathcal{D}_{\mathbf{v}_0} \subset \mathcal{D}_R(t, \beta_R)$.

Proof of (7.4). The proof of the last lower bound is more complicated than the previous ones. Specifically, we need to construct mixture distributions that reflect the uncertainty of both the first right and the first left singular vectors of Θ . Throughout, we set $\Pi = \mathbf{I}$.

Recall that $\beta_R \in [c_1 p^{-1/2} \sqrt{\log p}, 1]$. We define the following class of density P_Y of $Y = \Theta + Z$, where $Z_{ij} \sim_{i.i.d.} N(0, \sigma^2)$ and $\Theta = \lambda \mathbf{u} \mathbf{v}^\top$ for some fixed unit vectors $\mathbf{u} \in \mathbb{R}^n$ and $\mathbf{v} \in \mathbb{R}^p$ with some constraints, i.e.,

$$\mathcal{P}_{\mathbf{u}, t, \beta_R} = \left\{ P_Y : \begin{aligned} &Y = \Theta + Z, \Theta = \lambda \mathbf{u} \mathbf{v}^\top, \frac{\beta_R}{36} \leq \frac{v_{(p)} - \bar{v}}{V^{1/2}(\mathbf{v})} \leq \beta_R, \\ &t \leq \lambda \leq 6t, \|\mathbf{u}\|_2 = \|\mathbf{v}\|_2 = 1 \end{aligned} \right\}.$$

where for $\mathbf{x} = (x_1, \dots, x_p)$, we denote $\bar{x} = p^{-1} \sum_{j=1}^p x_j$, $V(\mathbf{x}) = \sum (x_i - \bar{x})^2$ and $x_{(p)}$ is the largest component of \mathbf{x} . In particular, the permutation matrix Π amounts to permuting the relative orders of the coordinates of \mathbf{v} , which is a monotone vector before permutation. In addition, for

any $\mathbf{w} \in \mathbb{R}^{p-1}$, define

$$\mathbf{w}_+ = \begin{bmatrix} \mathbf{w} \\ \frac{\beta_R}{4} \end{bmatrix} \in \mathbb{R}^p, \quad (7.12)$$

and define $\mathcal{U} = \{\mathbf{u} \in \mathbb{R}^n : |u_j| = 1/\sqrt{n}\}$. Denote

$$\mathcal{G} = \{\mathbf{w} \in \mathbb{R}^{p-1} : 1/2 \leq \|\mathbf{w}\|_2 \leq 2, \max\{w_{(p)}, |\bar{w}|\} \leq \frac{c_1}{8} p^{-1/2} \sqrt{\log p}\},$$

where $w_{(p)}$ is the largest component of \mathbf{w} . We construct the following Gaussian mixture measure

$$\begin{aligned} \bar{P}_{\mathbf{u}, t, \beta_R}(Y) &= C_{t, \beta_R} \int_{\mathcal{G}} \frac{\sigma^{np}}{(2\pi)^{np/2}} \exp(-\|Y - 2t\mathbf{u}\mathbf{w}_+^\top\|_F^2 / (2\sigma^2)) \\ &\quad \times \left(\frac{p-1}{2\pi}\right)^{(p-1)/2} \exp(-(p-1)\|\mathbf{w}\|_2^2 / 2) d\mathbf{w} \end{aligned}$$

Here C_{t, β_R} is the constant which normalizes the integral and makes $\bar{P}_{\mathbf{u}, t, \beta_R}$ a valid probability density. To be specific,

$$C_{t, \beta_R}^{-1} = P(\mathbf{w} \in \mathcal{G} | w_j \sim N(0, (p-1)^{-1}), 1 \leq j \leq p-1).$$

Moreover, since in the event \mathcal{G} , $2t\mathbf{u}\mathbf{w}_+^\top$ is rank one with the singular value $2t\|\mathbf{w}_+\|_2 \in (t, 2\sqrt{5}t)$ and by construction

$$\frac{\beta_R}{36} \leq \frac{w_{+, (p)} - \bar{w}_+}{V^{1/2}(\mathbf{w}_+)} \leq \beta_R,$$

it follows that $\bar{P}_{\mathbf{u}, t, \beta_R}(Y)$ is a mixture density of infinite members of $\mathcal{P}_{\mathbf{u}, t, \beta_R}$, i.e., $\bar{P}_{\mathbf{u}, t, \beta_R}(Y) \in \text{Conv}(\mathcal{P}_{\mathbf{u}, t, \beta_R})$.

The rest of the proofs rely on the our general lower bound based on testing multiple composite hypotheses (Lemma 2.2), as well as the following lemma that gives an upper bound for the KL-divergence between $\bar{P}_{\mathbf{u}, t, \beta_R}$ and $\bar{P}_{\mathbf{u}', t, \beta_R}$ for any $\mathbf{u}, \mathbf{u}' \in \mathbb{R}^n$.

Lemma 7.5. *Under the assumption of Proposition 7.1 (iii), for any unit vectors $\mathbf{u}, \mathbf{u}' \in \mathbb{R}^n$, we have*

$$D(\bar{P}_{\mathbf{u}, t, \beta_R} \| \bar{P}_{\mathbf{u}', t, \beta_R}) \leq \frac{C_1 t^4}{\sigma^2(4t^2 + \sigma^2(p-1))} (1 - (\mathbf{u}^\top \mathbf{u}')^2) + C_2$$

where $C_1, C_2 > 0$ are some uniform constant.

Again by Lemma 7.4, for any $\alpha, \epsilon \in (0, 1)$, there exists $\mathbf{u}_1, \dots, \mathbf{u}_m \in B(\mathbf{u}_0, \epsilon)$, such that $m \geq (c/\alpha)^{n-1}$ and $\min_{1 \leq i \neq j \leq m} \sqrt{1 - (\mathbf{u}_i^\top \mathbf{u}_j)^2} \geq \alpha\epsilon$. Again, we choose $\mathbf{u}_1, \dots, \mathbf{u}_m$ such that $\mathbf{u}_i^\top \mathbf{u}_j \geq 0$ for all $i, j \in \{1, \dots, m\}$. Hence, for $i = 1, \dots, m$, let μ_i be the priors over the parameter space of Θ leading to the posterior $\bar{P}_{\mathbf{u}_i, t, \beta_R}$. It holds that, for any $\Theta_i \in \text{supp}(\mu_i)$ and $\Theta_j \in \text{supp}(\mu_j)$ with

$1 \leq i \neq j \leq m$,

$$\|F(\Theta_i) - F(\Theta_j)\|_2 \geq C\|tu_i\beta_R - tu_j\beta_R\|_2 \geq Ct\beta_R\sqrt{2(1 - u_i^\top u_j)} \geq Ct\beta_R\alpha\epsilon,$$

and the KL-divergence $\max_{1 \leq i \leq m} D(P_{\mathbf{u}_i, t, \beta_R} \| P_{\mathbf{u}_0, t, \beta_R}) \leq \frac{C_1 t^4 \epsilon^2}{\sigma^2(4t^2 + \sigma^2(p-1))} + C_2$. Now set $\epsilon^2 = c(\frac{\sigma^2 n(t^2 + \sigma^2 p)}{t^4} \wedge 1)$ for some constant $c > 0$. Lemma 2.2 and the Markov inequality yield

$$\inf_{\hat{\Theta}} \sup_{\text{supp}(\mu_0), \dots, \text{supp}(\mu_m)} \mathbb{E}\|\hat{\Theta} - \Theta_R\|_2 \gtrsim t\beta_R \left(\frac{\sigma \sqrt{(t^2 + \sigma^2 p)n}}{t^2} \wedge 1 \right), \quad (7.13)$$

where the supremum is over the union of all the sets $\{\text{supp}(\mu_i)\}_{i=0}^m$. Finally, since $\cup_{i=0}^m \text{supp}(\mu_i) \times \{id\} \subset \mathcal{D}_R(t, \beta_R)$, equation (7.4) holds. \square

Proof of Theorem 4.1. Let $\hat{\Pi}$ be the permutation matrix corresponding to the permutation $\hat{\pi}$. For $i = 1, \dots, n$, we have $\check{Y}_i = (y_{i, \hat{\pi}(1)}, \dots, y_{i, \hat{\pi}(p)}) = Y_i \hat{\Pi}^{-1}$. Similarly, $(\hat{v}_{\hat{\pi}(1)}, \hat{v}_{\hat{\pi}(2)}, \dots, \hat{v}_{\hat{\pi}(p)}) = \hat{v}^\top \hat{\Pi}^{-1}$. Fitting a simple linear regression between \check{Y}_i and $(\hat{v}_{\hat{\pi}(1)}, \hat{v}_{\hat{\pi}(2)}, \dots, \hat{v}_{\hat{\pi}(p)})$ is therefore the same as fitting a regression between Y_i and \hat{v}^\top . As a result, if we denote $m(\hat{v}) = \frac{1}{p} \sum_{j=1}^p \hat{v}_j$, then

$$\beta_i = \frac{\sum_{j=1}^p (\hat{v}_j - m(\hat{v}))(y_{ij} - \bar{y}_i)}{\sum_{j=1}^p (\hat{v}_j - m(\hat{v}))^2} = \frac{\sum_{j=1}^p \hat{v}_j (y_{ij} - \bar{y}_i)}{\sum_{j=1}^p (\hat{v}_j - m(\hat{v}))^2} = \frac{\hat{v}^\top X_i}{\sum_{j=1}^p (\hat{v}_j - m(\hat{v}))^2},$$

and

$$\alpha_i = \bar{Y}_i - m(\hat{v})\beta_i = \frac{1}{p} \mathbf{e}^\top Y_i - m(\hat{v})\beta_i.$$

Hence

$$\hat{\Theta}_R^{Reg} = \frac{(\hat{v}_{(p)} - m(\hat{v}))X\hat{v}}{\sum_{j=1}^p (\hat{v}_j - m(\hat{v}))^2} + \frac{1}{p} Y \mathbf{e} = \frac{(\hat{v}_{(p)} - m(\hat{v}))X\hat{v}}{1 - pm^2(\hat{v})} + \frac{1}{p} Y \mathbf{e}. \quad (7.14)$$

Now recall that $X = Y(I_p - \frac{1}{p} \mathbf{e} \mathbf{e}^\top)$ so that $X \mathbf{e} = 0$. By SVD of X , each right singular vector of X is orthogonal to \mathbf{e} , so that $\hat{v}^\top \mathbf{e} = pm(\hat{v}) = 0$. Plugging $m(\hat{v}) = 0$ to (7.14), we have

$$\hat{\Theta}_R^{Reg} = X\hat{v} + \frac{1}{p} Y \mathbf{e} = \hat{\Theta}_R.$$

Similar arguments can be applied to prove $\hat{\Theta}_L^{Reg} = \hat{\Theta}_L$ and $\hat{\mathbf{R}}^{Reg} = \hat{\mathbf{R}}$.

FUNDING

This research was supported by NIH grants R01GM123056 and R01GM129781 and NSF grant DMS-1712735.

SUPPLEMENTARY MATERIALS

In our Supplemental Material (Ma et al., 2019b), we prove all the other theorems and relevant lemmas.

References

- Abel, S., P. A. Zur Wiesch, H.-H. Chang, B. M. Davis, M. Lipsitch, and M. K. Waldor (2015). Sequence tag-based analysis of microbial population dynamics. *Nature Methods* 12(3), 223.
- Boulund, F., M. B. Pereira, V. Jonsson, and E. Kristiansson (2018). Computational and statistical considerations in the analysis of metagenomic data. In *Metagenomics*, pp. 81–102. Elsevier.
- Bremer, H. and G. Churchward (1977). An examination of the cooper-helmstetter theory of dna replication in bacteria and its underlying assumptions. *Journal of Theoretical Biology* 69(4), 645–654.
- Brown, C. T., M. R. Olm, B. C. Thomas, and J. F. Banfield (2016). Measurement of bacterial replication rates in microbial communities. *Nature Biotechnology* 34(12), 1256.
- Brown, L. D. and E. Greenshtein (2009). Nonparametric empirical bayes and compound decision approaches to estimation of a high-dimensional vector of normal means. *The Annals of Statistics*, 1685–1704.
- Cai, T. T. and M. G. Low (2011). Testing composite hypotheses, hermite polynomials and optimal estimation of a nonsmooth functional. *The Annals of Statistics* 39(2), 1012–1041.
- Cai, T. T., Z. Ma, and Y. Wu (2013). Sparse pca: Optimal rates and adaptive estimation. *The Annals of Statistics* 41(6), 3074–3110.
- Cai, T. T. and A. Zhang (2018). Rate-optimal perturbation bounds for singular subspaces with applications to high-dimensional statistics. *The Annals of Statistics* 46(1), 60–89.
- Carpentier, A. and T. Schlueter (2016). Learning relationships between data obtained independently. *arXiv preprint arXiv:1601.00504*.
- Chatterjee, S., A. Guntuboyina, and B. Sen (2015). On risk bounds in isotonic and other shape restricted regression problems. *The Annals of Statistics* 43(4), 1774–1800.
- Chatterjee, S., A. Guntuboyina, and B. Sen (2018). On matrix estimation under monotonicity constraints. *Bernoulli* 24(2), 1072–1100.
- Cooper, S. and C. E. Helmstetter (1968). Chromosome replication and the division cycle of escherichia coli b/r. *Journal of Molecular Biology* 31(3), 519–540.

- Copas, J. (1969). Compound decisions and empirical bayes. *Journal of the Royal Statistical Society: Series B (Methodological)* 31(3), 397–417.
- Flammarion, N., C. Mao, and P. Rigollet (2019). Optimal rates of statistical seriation. *Bernoulli* 25(1), 623–653.
- Gao, F., H. Luo, and C.-T. Zhang (2013). Doric 5.0: an updated database of oric regions in both bacterial and archaeal genomes. *Nucleic Acids Research* 41, D90.
- Gao, Y. and H. Li (2018). Quantifying and comparing bacterial growth dynamics in multiple metagenomic samples. *Nature Methods* 15, 1041–1044.
- Korem, T., D. Zeevi, J. Suez, A. Weinberger, T. Avnit-Sagi, M. Pompan-Lotan, E. Matot, G. Jona, A. Harmelin, and N. Cohen (2015). Growth dynamics of gut microbiota in health and disease inferred from single metagenomic samples. *Science*, aac4812.
- Langmead, B. and S. L. Salzberg (2012). Fast gapped-read alignment with bowtie 2. *Nature Methods* 9(4), 357.
- Li, D., C.-M. Liu, R. Luo, K. Sadakane, and T.-W. Lam (2015). Megahit: an ultra-fast single-node solution for large and complex metagenomics assembly via succinct de bruijn graph. *Bioinformatics* 31(10), 1674–1676.
- Li, H., B. Handsaker, A. Wysoker, T. Fennell, J. Ruan, N. Homer, G. Marth, G. Abecasis, and R. Durbin (2009). The sequence alignment/map format and samtools. *Bioinformatics* 25(16), 2078–2079.
- Lloyd-Price, J., C. Arze, A. N. Ananthakrishnan, M. Schirmer, J. Avila-Pacheco, T. W. Poon, E. Andrews, N. J. Ajami, K. S. Bonham, C. J. Brislawn, et al. (2019). Multi-omics of the gut microbial ecosystem in inflammatory bowel diseases. *Nature* 569(7758), 655.
- Ma, R., T. T. Cai, and H. Li (2019a). Optimal permutation recovery in permuted monotone matrix model. *arXiv preprint arXiv:1911.10604*.
- Ma, R., T. T. Cai, and H. Li (2019b). Supplement to “optimal and adaptive estimation of extreme values in the permuted monotone matrix model”.
- Mao, C., A. Pananjady, and M. J. Wainwright (2018). Towards optimal estimation of bivariate isotonic matrices with unknown permutations. *arXiv preprint arXiv:1806.09544*.
- Massart, P. (2007). *Concentration Inequalities and Model Selection: Ecole d’Eté de Probabilités de Saint-Flour XXXIII-2003*. Springer.

- Myhrvold, C., J. W. Kotula, W. M. Hicks, N. J. Conway, and P. A. Silver (2015). A distributed cell division counter reveals growth dynamics in the gut microbiota. *Nature Communications* 6, 10039.
- Rigollet, P. and J. Weed (2018). Uncoupled isotonic regression via minimum wasserstein deconvolution. *arXiv preprint arXiv:1806.10648*.
- Robbins, H. (1951). Asymptotically subminimax solutions of compound statistical decision problems. In *Proceedings of the 2nd Berkeley Symposium on Mathematical Statistics and Probability*. The Regents of the University of California.
- Robbins, H. (1964). The empirical bayes approach to statistical decision problems. *The Annals of Mathematical Statistics* 35(1), 1–20.
- Samuel, E. (1967). The compound statistical decision problem. *Sankhyā: The Indian Journal of Statistics, Series A*, 123–140.
- Szarek, S. J. (1982). Nets of grassmann manifold and orthogonal group. In *Proceedings of Research Workshop on Banach Space Theory (Iowa City, Iowa, 1981)*, Volume 169, pp. 185.
- Tsybakov, A. B. (2009). *Introduction to Nonparametric Estimation*. Springer Series in Statistics. Springer, New York.
- Vershynin, R. (2010). Introduction to the non-asymptotic analysis of random matrices. *arXiv preprint arXiv:1011.3027*.
- von Meijenfeldt, F. B., K. Arkhipova, D. D. Cambuy, F. H. Coutinho, and B. E. Dutilh (2019). Robust taxonomic classification of uncharted microbial sequences and bins with cat and bat. *bioRxiv*, 530188.
- Wu, Y.-W., B. A. Simmons, and S. W. Singer (2015). Maxbin 2.0: an automated binning algorithm to recover genomes from multiple metagenomic datasets. *Bioinformatics* 32(4), 605–607.
- Yu, B. (1997). Assouad, fano, and le cam. In *Festschrift for Lucien Le Cam*, pp. 423–435. Springer.
- Zhang, A., T. T. Cai, and Y. Wu (2018). Heteroskedastic pca: Algorithm, optimality, and applications. *arXiv preprint arXiv:1810.08316*.
- Zhang, A. and Y. Zhou (2018). A non-asymptotic, sharp, and user-friendly reverse chernoff-cramér bound. *arXiv preprint arXiv:1810.09006*.
- Zhang, C.-H. (2003). Compound decision theory and empirical bayes methods. *The Annals of Statistics* 31(2), 379–390.

A Supplementary Tables and Figures

We summarize our supplementary tables and figures as follows:

1. In Table S.1, we provide the complete taxonomic annotations of the five differential bins identified from the F test in Section 5.3 of the main paper.
2. In Figure 5, we provide the boxplots of the ePTRs of the above five differential bins.

Table S.1: The complete taxonomic annotations with lineage scores indicating the quality of each taxonomic classification.

Bins	Taxonomic Annotations with Lineage Scores
bin.054	Firmicutes (phylum): 0.98; Clostridia (class): 0.97; Clostridiales (order): 0.97 Lachnospiraceae (family): 0.93; Roseburia (genus): 0.92
bin.090	Firmicutes (phylum): 0.97; Clostridia (class): 0.95; Clostridiales (order): 0.95; Ruminococcaceae (family): 0.84; Faecalibacterium (genus): 0.82
bin.091	Firmicutes (phylum): 0.95; Clostridia (class): 0.93; Clostridiales (order): 0.93
bin.099	Firmicutes (phylum): 0.96; Clostridia (class): 0.94; Clostridiales (order): 0.94; Ruminococcaceae (family): 0.87; Subdoligranulum (genus): 0.76; Subdoligranulum sp. APC924/74 (species): 0.74
bin.465	Firmicutes (phylum): 0.98; Negativicutes (class): 0.97; Veillonellales (order): 0.96; Veillonellaceae (family): 0.96; Dialister (genus): 0.94

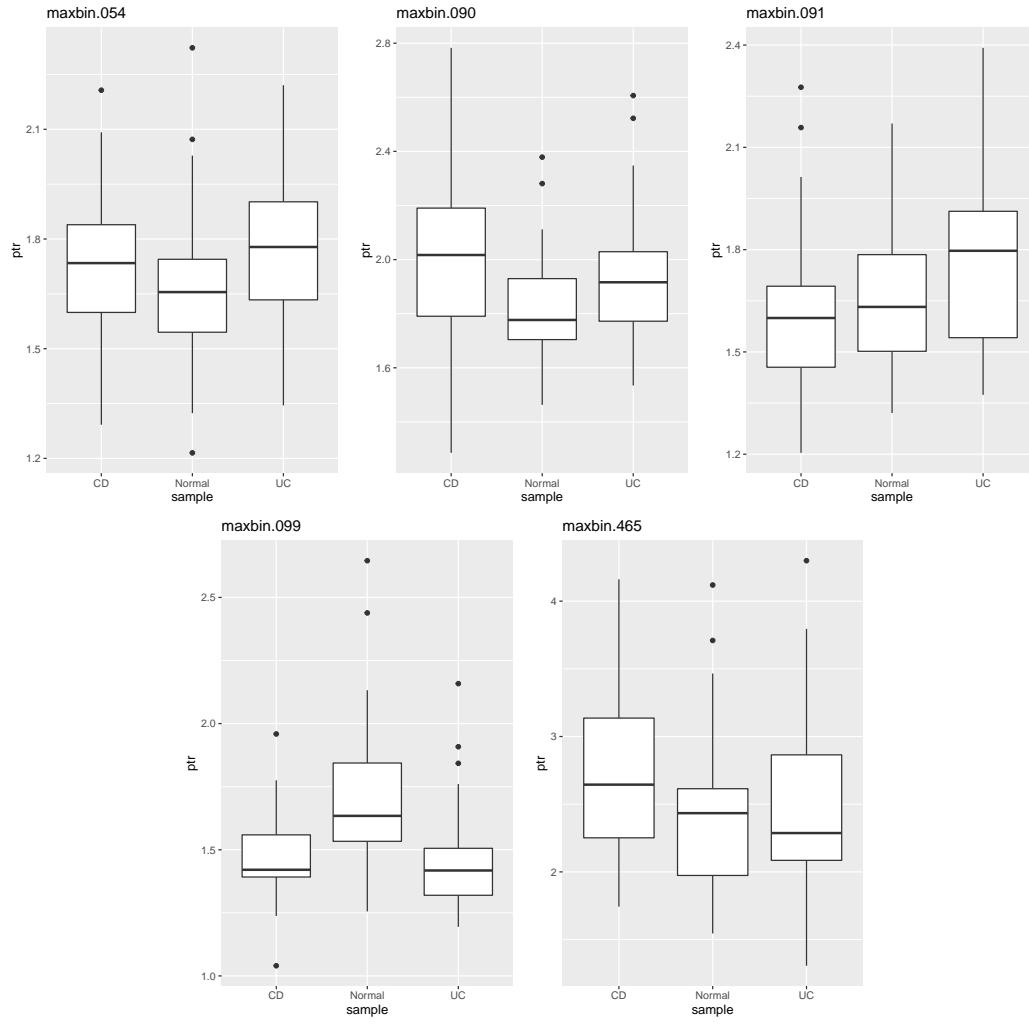


Figure 5: Boxplots of the ePTRs of the five differential bins identified from the F test